Hindawi
Journal of Advanced Transportation
Volume 2018, Article ID 5427507, 26 pages
https://doi.org/10.1155/2018/5427507

Research Article

An Extended Car-Following Model at Signalised Intersections

Hongxing Zhao, Ruichun He, and Changxi Ma

School of Traffic and Transportation, Lanzhou Jiaotong University, Lanzhou 730070, China

Correspondence should be addressed to Ruichun He; tranman@163.com

Received 10 April 2018; Revised 19 June 2018; Accepted 11 July 2018; Published 25 July 2018

Academic Editor: Antonio Comi

An extended car-following model is proposed on the basis of experimental analysis to improve the performance of the traditional car-following model and simulate a microscopic car-following behaviour at signalised intersections. The new car-following model considers vehicle gather and dissipation. Firstly, the parameters of optimal velocity, generalised force and full velocity difference models are calibrated by measured data, and the problems and causes of the three models are analysed with a realistic trajectory simulation as an evaluation criterion. Secondly, an extended car-following model based on the full optimal velocity model is proposed by considering the vehicle gather and dissipation. The parameters of the new car-following model are calibrated by the measured data, and the model is compared with comparative models on the basis of isolated point data and the entire car-following process. Simulation results show that the optimal velocity, generalised force, and full velocity difference models cannot effectively simulate a microscopic car-following behaviour at signalised intersections, whereas the new car-following model can avoid a collision and has a high fit degree for simulating the measured data of the car-following behaviour at signalised intersections.

1. Introduction

A car-following model is a mathematical description of the movement of a car in the same lane given the change in the moving state of the front car under the case of no overtaking; this model is also a link or bridge between macroscopic traffic flow theory and microscopic traffic flow model [1]. In recent years, an increasing number of mathematical models on car-following behaviour have been developed on the basis of experimental observations and theoretical analyses; the cornerstone for simulation modelling and traffic control, including early linear models proposed by Chandler et al. [2] and Herman et al. [3] and nonlinear models by Reuschel [4], Pipes [5], Gazis et al. [6], Newell [7], Bando et al. [8], Helbing and Tilch [9], and Jiang et al. [10], has been established. Chandler et al. [2] proposed the first prototype car-following model in 1958 at the General Motors Research Laboratory. This model was based on an intuitive hypothesis that the acceleration of a driver is proportional to the relative velocity of the front car. An initial calibration of this model used wire-linked vehicles to examine the responses of eight test subjects to a 'realistic' speed profile of a lead vehicle for 30 min on a test track. A rapid development of this model subsequently followed; Herman et al. [3] studied local and asymptotic stabilities of traffic flow in the fleet and discussed the influence of subadjacent leading vehicle car-following behaviour. Reuschel [4] and Pipes [5] first used analytical methods to study the problem of car-following behaviour; many subsequent models were developed from the Pipes model. Gazis et al. [6] discussed various nonlinear follow-the-leader models of traffic flow given available observational and experimental data that focus on steady-state flow equations. Newell [7] believed that the stimulus of a driver originates from the headway but not the relative speed; thus, Newell proposed a nonlinear car-following model with the headway as a stimulus. An optimal velocity (OV) model proposed by Bando et al. [8] is a favourable car-following model because it can describe many properties of actual traffic flow, such as instability of traffic flow, evolution of traffic congestion, and formation of stop-and-go waves. However, a comparison of empirical data indicates that the OV model exhibits significantly high acceleration and unrealistic deceleration; Helbing and Tilch [9] proposed a generalised force (GF) model by considering the negative velocity difference to overcome the abovementioned limitation. The simulation showed that the GF model is poor in the delay time of a car motion; owing to this problem, Jiang et al. [10] modified the model in 2001 by considering the negative and positive velocity differences and developed a full velocity difference (FVD) model. Subsequently, many similar works have been performed by several other authors [11–43].

The exploration of an urban signal intersection is important in traffic flow research because it can provide a theoretical basis for intersection signal timing. In recent years, the research on traffic flow theory of signal intersection has also gained certain favourable results. Sasaki and Nagatani [44] used the OV model to study traffic flow controlled by traffic lights on a single-lane roadway and found that the saturation of current occurs at the critical density; moreover, the critical density of a dynamical transition depends on the cycle time of the traffic light and strategy. Tang et al. [45] analysed the car-following behaviour in a road traffic system that contains signal lights and presented a traffic flow model that considers the signal light influence. However, the two models have not been calibrated or verified using the measured data; therefore, Yu et al. [46–49] proposed the car-following model which considers the influence of a signal lamp on the basis of the experimental analysis; the measured data were mined to find endogenous variables as the input variables of the car-following model by using a grey correlation analysis method; then, various extended car-following models were proposed on the basis of the FVD model; the results of the numerical simulations indicated that the extended car-following models can improve traffic flow stability. Fitting verification through the measured data remains lacking despite various car-following models that consider the influence of signal lamps in the literature [46–49]. Subsequently, Yu and Shi [50] used the OV and GF models to simulate the car-following behaviour at signalised intersections on the basis of the simulation system that analyses the problems and their causes; a new car-following model was proposed, and a fitting verification was conducted on the basis of the measured data. Similarly, Li and Yu [51] proposed a new model and improved the fit degree of the car-following model to the actual trajectory of the vehicle.

In summary, many important research results have been achieved on the car-following model. However, analysing a car-following behaviour at signalised intersections and studying the adaptability of the car-following models to vehicle trajectory simulations are limited. The measured data are used to calibrate the related car-following model and conduct the fitting analysis in the literature [50, 51], and the new car-following model at signalised intersections is proposed on the basis of the analysis results; however, only the car-following behaviours of the gather vehicles is considered, whereas those of the dissipated vehicles are disregarded. Thus, studying the car-following model at signalised intersections remains necessary, especially based on measured data; moreover, a new car-following model with a high fit degree must be proposed. In contrast to the literature [50, 51], the present study verifies the fit of the OV, GF, and FVD models for the measured car-following behaviour, analyses existing problems and their causes, and proposes a new car-following model on the basis of the measured data by considering the vehicle gather and dissipation behaviours.

The remainder of this paper is organised as follows. The data sources are introduced in Section 2. The analysis results of the OV, GF, and FVD models are presented in Section 3. An extended car-following model at signalised intersections is proposed in Section 4. A comparative analysis is conducted and then discussed in Section 5 to illustrate the effectiveness of the improved car-following model. Finally, the paper is summarised, and conclusions are drawn in Section 6.

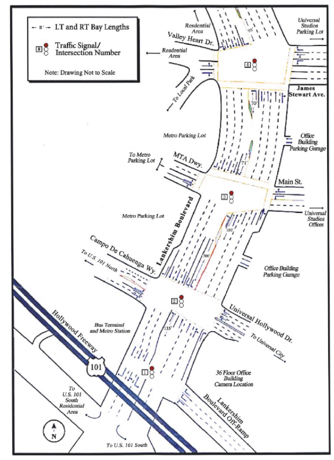

Figure 1: Study area: Lankershim Boulevard, where 101 is US Highway 101, and 1, 2, 3, and 4 are the intersection numbers.

2. Data Source

The Federal Highway Administration (FHWA) has been a leader in developing traffic simulation models since the 1970s. Commercial traffic simulation packages remained lacking in the marketplace before the FHWA assumed a leadership role. The Traffic Analysis Tools Programme of the FHWA launched the Next Generation SIMulation (NGSIM) programme to help achieve an extensive acceptance of using microsimulation systems and ensure that the tools provide accurate results. The data for the simulation analysis used in the present study are derived from the NGSIM programme, and the US Highway Agency provides the data free of charge [52]. Lankershim Boulevard dataset was collected under the NGSIM programme. The researchers for the NGSIM programme collected detailed vehicle trajectory data from Lankershim Boulevard in the Universal City neighbourhood of Los Angeles, CA, on 16 June 2005. The study area, as illustrated in Figure 1, consisted of bidirectional data of three- to four-lane arterial segments and a complete coverage of three signalised intersections; the study area is approximately 500 m in length. The Lankershim Boulevard dataset was selected as the data source. Data acquisition period is from 8:30 a.m. to 9:00 a.m.; at this time, the traffic state has just recovered from the morning to flat peak, the traffic density is relatively moderate, and the car-following behaviour is widespread and has robust representativeness. These data were collected using five video cameras mounted on the roof of a high building, and the vehicle trajectory data were transcribed from the video through NG-VIDEO, a customised software application that was developed for the NGSIM programme and recorded in the database.

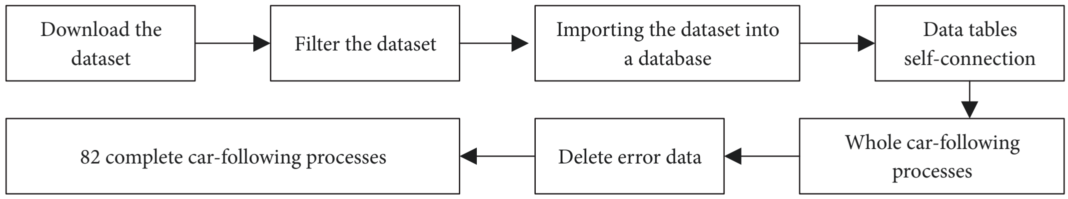

Figure 2: Data processing flow.

These vehicle trajectory data provided the precise location of each vehicle within the study area every one-tenth of a second. The data include solid-state information, such as vehicle number, type, width and length, and dynamic information, such as vehicle lane, intersection number, leading vehicle number, following vehicle number, acceleration, speed, distance headway, and global time. The vehicle number is the unique identification of each vehicle. We can determine the change in the position and motion state in the continuous time and then determine the relatively complete car-following process through the vehicle number and time information. The data of the car-following process can be divided into the road and intersection. The present study focuses on the car-following model at signalised intersections. The dataset must be processed to obtain the data required for this study. The data processing flow is illustrated in Figure 2. Firstly, we filtered the data that did not accumulate near the intersection on the basis of the intersection number. Then, we imported the filtered dataset into the database. Furthermore, we built a self-connection of data tables on the basis of the intersection number, leading vehicle number, following vehicle number and global time, and thereby obtaining numerous complete car-following processes. On this basis, we deleted the car-following process that had apparent errors in the dataset. Examples of these errors included the following: vehicle distance headway was less than 5 m, and the leading or following vehicle had unreasonable acceleration/deceleration and velocity. Then, we obtained 82 complete car-following processes that included 3,924 isolated point data. The data of the two car-following processes are summarised in Table 1. The data in Table 1 include only the car-following track for every 0.5 s given the limited length of this paper. In Table 1, $a_{n-1}(t)$ is the acceleration/deceleration of the $n-1$th car, that is, the leading car at time t; $v_{n-1}(t)$ is the velocity of the $n-1$th car at time t; $a_n(t)$ is the acceleration/deceleration of the *nth* car, that is, the following car at time t; $v_n(t)$ is the velocity of the nth at time t; $\Delta x_n(t)$ is the distance headway between the nth car and its leading car $n-1$ at time t. At the signal intersection, the vehicle cannot traverse the intersection smoothly, the vehicle decelerates, and the idle speed is maintained for a certain period. Then, the vehicle speeds away from the intersection when the red light is turned off and the green light is turned on. This phenomenon is called complete parking. Simultaneously, the vehicles that arrive during the green-light stage will decelerate given the influence of the queuing vehicles during the red-light stage and the queuing vehicles in front will accelerate. This phenomenon is called incomplete parking. In the two phenomena, the driver will have a different car-following behaviour. Thus, Processes 1 and 2 in Table 1 correspond to the situation of incomplete and complete parking, respectively, which are selected to represent the two types of car-following behaviour at the intersection. The two typical processes are simulated to judge the adaptability of the car-following model to analyse the car-following track.

3. Model Simulation and Analysis

The vehicle trajectory fitting simulation of the intersection is conducted on the basis of the OV, GF, and FVD models. The establishment of a traffic flow model will eventually return to the actual application. We can obtain a realistic model only by identifying the parameters of the model on the basis of numerous observations and an in-depth analysis of the actual traffic phenomenon. Thus, we randomly select 48 complete car-following processes that include 2626 isolated point data as learning samples to calibrate the model. Furthermore, the adaptive verification and analysis are conducted using the OV, GF, and FVD models which are calibrated by the actual car-following data.

3.1. OV Model. Bando et al. [8] proposed the OV model in 1995 to describe the car-following behaviour on a single-lane highway. The model was presented by introducing the OV function to optimise the OV in accordance with the distance headway. The motion formula is expressed as follows:

$$a_n(t) = \kappa \left(V\left(\Delta x_n(t)\right) - v_n(t) \right), \quad (1)$$

where $v_n(t)$ is the velocity of the nth car at time t; $\Delta x_n(t) = x_{n-1}(t) - x_n(t)$ is the distance headway between the nth car and its leading car $n-1$ at time t; $x_{n-1}(t)$ and $x_n(t)$ are the positions of the $n-1$th and nth cars, respectively; κ is the sensitivity parameter of the driver, and $V(\cdot)$ is the OV function which can be formulated as follows:

$$V\left(\Delta x_n(t)\right) = v_1 + v_2 \tanh\left(c_1\left(\Delta x_n(t) - l\right) - c_2\right), \quad (2)$$

where l is the vehicle length, and v_1, v_2, c_1, and c_2 are the parameters of the OV function that lacks physical meaning and must be calibrated.

Helbing et al. [9] calibrated the OV model, but the calibration data are obtained from the experimental site and are not the measured data at the signalised intersection. Thus, recalibrating the OV model by using the measured data of the car-following process at signalised intersections is required. The 2626 isolated point data are selected as learning samples, and the parameters of the OV model are calibrated

Table 1: Measured data of two typical car-following processes.

Car-following processes	Number of isolated points	$a_{n-1}(t)$ (m·s^{-2})	$v_{n-1}(t)$ (m·s^{-1})	$a_n(t)$ (m·s^{-2})	$v_n(t)$ (m·s^{-1})	$\Delta x_n(t)$ (m)
	1	-0.55	2.64	0.00	10.27	19.88
	2	-1.67	2.19	2.01	10.07	15.51
	3	0.95	1.97	-4.75	9.30	13.57
	4	-1.01	1.54	-5.65	6.98	10.45
	5	-1.19	1.16	-3.58	4.30	8.59
	6	1.52	0.94	-2.15	2.84	7.77
	7	-0.45	1.02	-1.85	1.34	7.40
1	8	-1.53	1.17	-1.03	1.23	7.32
	9	1.73	1.11	-1.29	1.16	7.33
	10	2.19	1.34	-0.52	1.44	7.24
	11	0.88	2.32	-0.74	1.06	7.54
	12	2.55	3.39	2.22	1.75	8.23
	13	2.93	4.54	2.31	2.33	9.13
	14	2.61	6.26	2.41	3.51	10.52
	15	3.62	8.01	2.62	5.23	11.91

TABLE 1: Continued.

Car-following processes	Number of isolated points	$a_{n-1}(t)$ ($m \cdot s^{-2}$)	$v_{n-1}(t)$ ($m \cdot s^{-1}$)	$a_n(t)$ ($m \cdot s^{-2}$)	$v_n(t)$ ($m \cdot s^{-1}$)	$\Delta x_n(t)$ (m)
	1	0.58	5.12	3.14	8.30	12.24
	2	-0.79	4.79	-3.62	5.41	9.91
	3	-2.97	3.88	-3.42	3.97	8.67
	4	-2.32	0.19	-2.26	1.33	7.87
	5	0.00	0.00	-1.99	0.45	7.66
	6	0.00	0.00	0.00	0.00	7.64
	7	0.00	0.00	0.00	0.00	7.64
	8	0.00	0.00	0.00	0.00	7.64
	9	0.00	0.00	0.00	0.00	7.64
	10	0.00	0.00	0.00	0.00	7.64
	11	0.00	0.00	0.00	0.00	7.64
	12	0.00	0.00	0.00	0.00	7.64
	13	0.00	0.00	0.00	0.00	7.64
	14	0.00	0.00	0.00	0.00	7.64
	15	0.00	0.00	0.00	0.00	7.64
	16	0.00	0.00	0.00	0.00	7.64
	17	0.00	0.00	0.00	0.00	7.64
	18	0.00	0.00	0.00	0.00	7.64
	19	0.00	0.00	0.00	0.00	7.64
	20	0.00	0.00	0.00	0.00	7.64
	21	0.00	0.00	0.00	0.00	7.64
	22	0.00	0.00	0.00	0.00	7.64
	23	0.00	0.00	0.00	0.00	7.64
	24	0.00	0.00	0.00	0.00	7.64
	25	0.00	0.00	0.00	0.00	7.64
	26	0.00	0.00	0.00	0.00	7.64
2	27	0.00	0.00	0.00	0.00	7.64
	28	0.00	0.00	0.00	0.00	7.64
	29	0.00	0.00	0.00	0.00	7.64
	30	0.00	0.00	0.00	0.00	7.64
	31	0.00	0.00	0.00	0.00	7.64
	32	0.00	0.00	0.00	0.00	7.64
	33	0.00	0.00	0.00	0.00	7.64
	34	0.00	0.00	0.00	0.00	7.64
	35	0.00	0.00	0.00	0.00	7.64
	36	0.00	0.00	0.00	0.00	7.64
	37	0.00	0.00	0.00	0.00	7.64
	38	0.00	0.00	0.00	0.00	7.64
	39	0.00	0.00	0.00	0.00	7.64
	40	0.00	0.00	0.00	0.00	7.64
	41	0.00	0.00	0.00	0.00	7.64
	42	0.00	0.00	0.00	0.00	7.64
	43	0.00	0.00	0.00	0.00	7.64
	44	0.00	0.00	0.00	0.00	7.64
	45	0.50	0.03	0.00	0.00	7.64
	46	1.84	1.36	0.00	0.00	8.10
	47	1.94	1.62	0.21	0.02	9.03
	48	3.57	4.50	-0.12	0.08	10.27
	49	1.27	5.03	3.48	1.25	11.62
	50	3.33	7.21	-0.25	2.41	13.50
	51	0.24	7.51	3.75	3.64	15.86
	52	1.42	8.58	3.19	7.56	17.00
	53	0.67	8.69	-3.39	8.29	17.97
	54	0.00	9.58	0.00	8.00	19.63

through the optimisation algorithm. In literature [50, 51, 53], particle swarm optimisation and genetic algorithms are used to calibrate the model, correspondingly. In contrast to literature [50, 51, 53], we select the standard artificial bee colony (ABC) algorithm which performs better than the other heuristic algorithms [54] in terms of calibrating the model.

The error between the actual and the simulated velocities can be used as the criterion of the consistency degree of the vehicle state in simulating the car-following process because the velocity can describe the running state of the vehicle in real time. The distance headway is the key parameter of the transition from the microscopic behaviour of a vehicle to the macroscopic phenomenon of the traffic flow. The error of the distance headway can directly reflect the consistency degree of the car-following phenomenon which is obtained by the individual vehicle on the basis of applying the OV model. Thus, the distance headway error should also be used as a criterion to evaluate the effect of the car-following model. That is, the mean absolute relative error of the velocity and the distance headway are considered, simultaneously, the optimisation criteria which can be formulated as follows:

$$EC = w_1 MARE(\Delta x) + w_2 MARE(v), \tag{3}$$

where w_1 and w_2 are the weight parameters. Simulating the microscopic behaviour of vehicles and analysing the macroscopic traffic phenomena are equally important because of the application of the car-following model for the analysis of the car-following behaviour at signalised intersection. That is, the distance headway and the velocity errors must be accorded with the same attention. Thus, we set w_1 and w_2 to 0.5 and 0.5, correspondingly. $MARE(\Delta x)$ and $MARE(v)$ correspond to the mean absolute relative error of the distance headway and the velocity and can be formulated as follows:

$$MARE(\Delta x) = \frac{1}{n}\sum_{i=1}^{n}\left|\frac{\Delta x - \Delta\hat{x}}{\Delta\hat{x}}\right|, \tag{4}$$

$$MARE(v) = \frac{1}{n}\sum_{i=1}^{n}\left|\frac{v - \hat{v}}{\hat{v}}\right|, \tag{5}$$

where n is the number of learning sample, Δx is the simulated distance headway of the OV model, $\Delta\hat{x}$ is the empirical distance headway, v is the simulated velocity of the OV model, and $\hat{v}$ is the empirical velocity.

The ABC algorithm is selected as the optimisation algorithm, and (3) can be minimised by optimising the parameters of the OV model. The number of employed, onlooker, and scout bees is set to 100, 100, and 1, respectively, and the maximum number of stagnation and the number of iteration in the ABC algorithm are set to 1600 and 3000, correspondingly. The same resulting parameters are obtained consistently through repeated analyses of the experiment. Moreover, the algorithm converges to these resulting parameters, and the number of first ABC iteration of the result is at most 2000 times. Thus, the algorithm has converged to the global optimal solution. The resulting parameters of the OV model are $\kappa = 0.70$, $v_1 = 2.04$, $v_2 = 1.99$, $c_1 = 18.07$, and $c_2 = 99.93$.

We selected two complete car-following processes, as presented in Table 1, to verify the adaptability of the calibrated OV model to the car-following trajectory at the signal intersection and test the OV model. In Table 1, the first point data of the two car-following process data are used as the initial state of the simulation. The complete simulation of the car-following process can then be obtained on the basis of the evolution of the model. The simulation results are depicted in Figures 3 and 4.

Figure 3(a) demonstrates the simulation analysis of the acceleration/deceleration of the OV model for car-following Process 1. This figure displays that the deceleration is faster than the measured data at the early deceleration stage, but the subsequent deceleration stage is slower than the measured data. Moreover, the simulation results of the OV model at the acceleration stage indicate a slow and insufficient acceleration over the measured data. Figure 3(b) exhibits the simulation analysis of the velocity of the OV model in car-following Process 1. This figure presents that the velocity of the early deceleration stage is less than the measured data, but the velocity of the subsequent deceleration stage is greater than the measured data. Moreover, the velocity of the OV model at the acceleration stage is less than the measured data. Figure 3(c) illustrates the simulation analysis of the distance headway of the OV model in car-following Process 1. This figure depicts that the distance headway of the entire deceleration stage is greater than the measured data given the significant deceleration at the early deceleration stage. The distance headway of the subsequent deceleration and early acceleration stages is greater than the measured data given the minimal deceleration at the succeeding deceleration stage. Furthermore, the simulation value of the distance headway for a period is close to 5 m given the minimal deceleration. Thus, the following car has the risk of a rear-end collision. The comprehensive analysis of Figures 3(a), 3(b), and 3(c) indicate the same results as those obtained through the simulation analysis of acceleration/deceleration, velocity, and distance headway. The OV model simulation of car-following Process 1 has the problem of significant deceleration at the early deceleration stage and minimal deceleration at the subsequent deceleration stage. Thus, the distance headway of the following car is approximately 5 m for a period, thereby resulting in the risk of rear-end collision for the following car. Furthermore, the OV model demonstrates a slow and insufficient acceleration over the measured data at the acceleration stage. Therefore, the fit degree is relatively low between the simulation and the measured trajectories when the OV model simulates car-following Process 1.

Figure 4(a) presents the simulation analysis of the acceleration/deceleration of the OV model in car-following Process 2. This figure shows that the deceleration is slower than the measured data at the deceleration stage, and the problem of the OV model simulation of car-following Process 2 at the acceleration stage is consistent with that of car-following Process 1. The simulation results of the OV model show slow and insufficient acceleration over the measured data. Figure 4(b) illustrates the simulation analysis of the velocity of the OV model in car-following Process 2. This figure depicts that the velocity is greater in the deceleration stage than

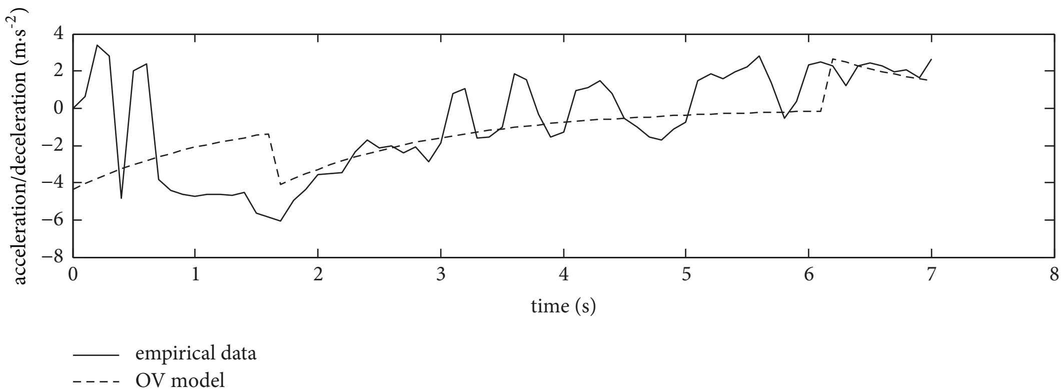

(a) Simulation of acceleration/deceleration

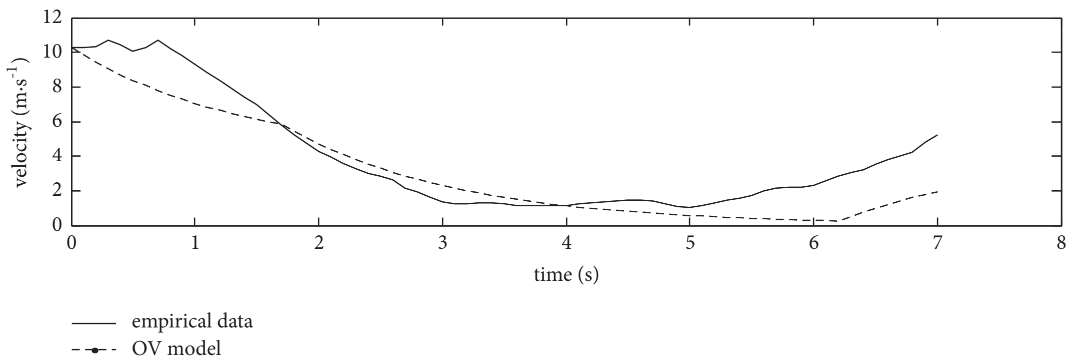

(b) Simulation of velocity

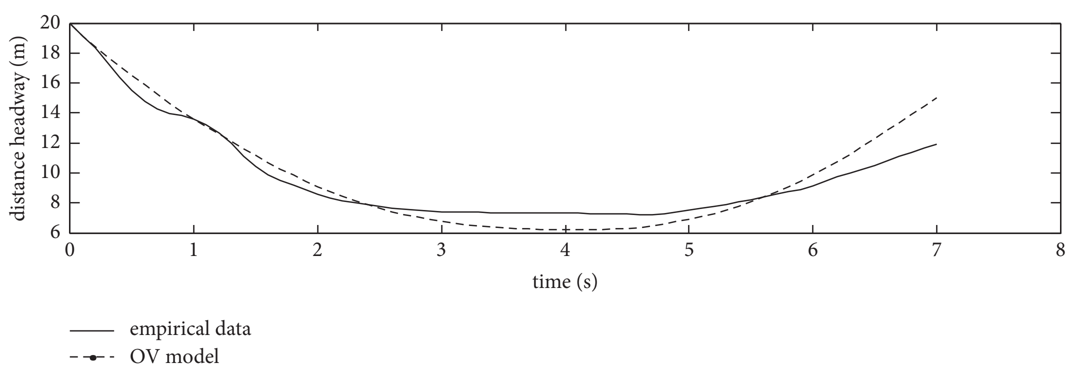

(c) Simulation of distance headway

Figure 3: OV model simulations of car-following Process 1.

in the measured data, and the problem of the OV model simulation of car-following Process 2 at the acceleration stage is consistent with that of car-following Process 1. Moreover, the velocity is less in the OV model than in the measured data. Figure 4(c) depicts the simulation analysis of the distance headway of the OV model in car-following Process 2. This figure illustrates that the distance headway of the following car is less than 5 m in the entire idling stage given the minimal deceleration at the deceleration stage, thereby causing a risk of a rear-end collision for the following car. Furthermore, the distance headway at the acceleration stage is greater in the OV model than in the measured data given the minimal acceleration. The comprehensive analyses of Figures 4(a), 4(b), and 4(c) depict the same results as those obtained through the simulation analysis of acceleration/deceleration, velocity, and distance headway. The OV model simulation of car-following Process 2 shows a minimal deceleration at the deceleration stage. Thus, the distance headway of the following car is less than 5 m in the entire idling stage, thereby resulting in a rear-end collision of the following car. The OV model shows a slow and insufficient acceleration over the measured data at the acceleration stage. Therefore, the fit degree is relatively low between the simulation and the measured trajectories when the OV model simulates car-following Process 2.

The results of the simulation analysis of car-following Processes 1 and 2 using the OV model show that the OV model simulation of the gather vehicle has a minimal

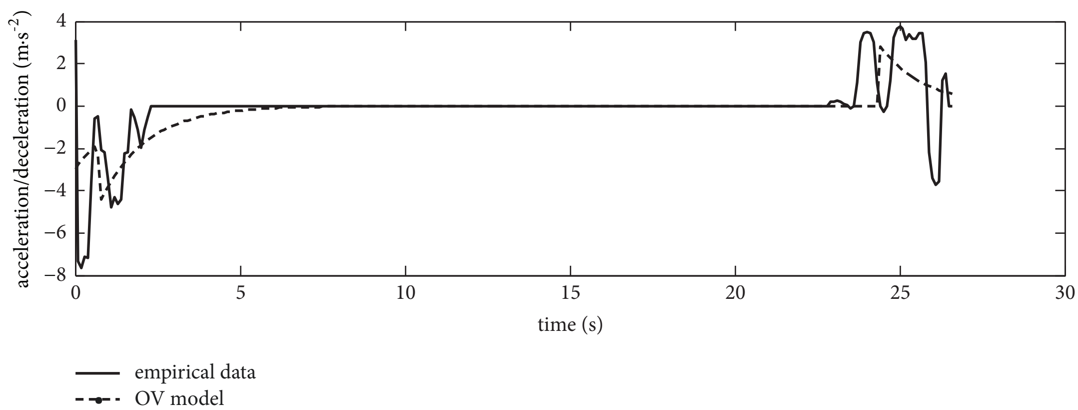

(a) Simulation of acceleration/deceleration

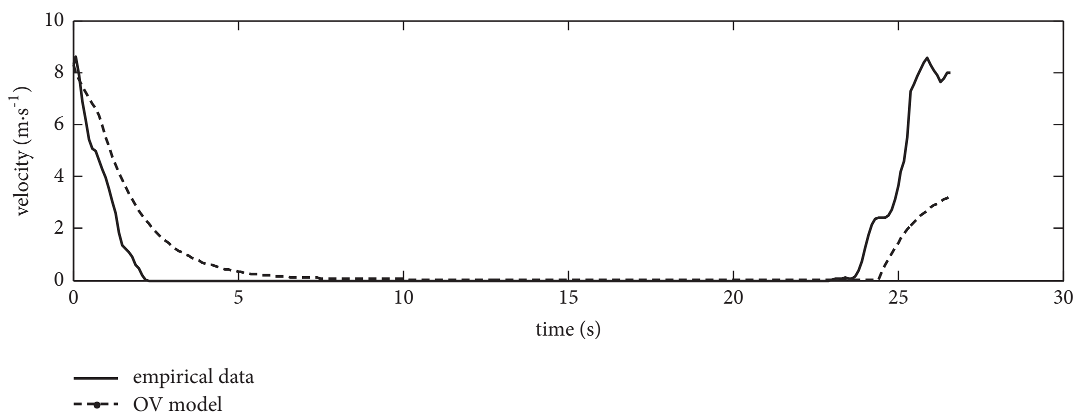

(b) Simulation of velocity

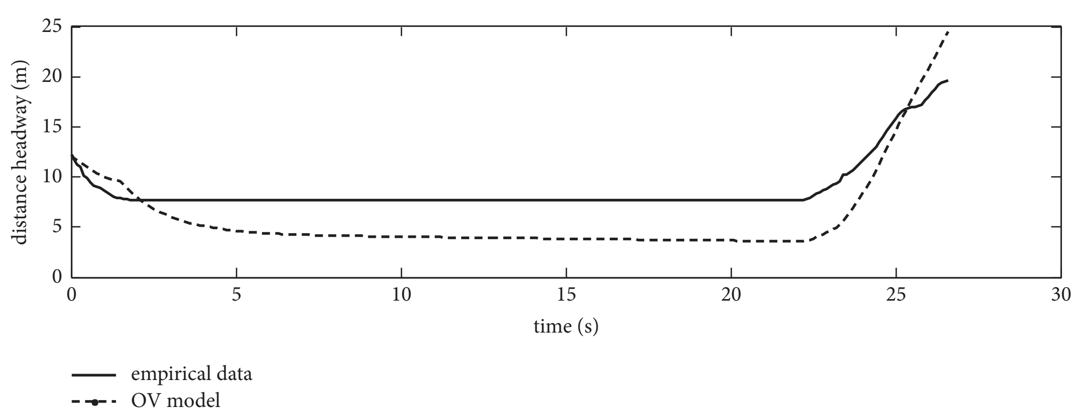

(c) Simulation of distance headway

Figure 4: OV model simulations of car-following Process 2.

deceleration at the deceleration stage, thereby causing the following car to be subjected to the risk of a rear-end collision. The OV model simulation of the dissipation vehicle has a slow acceleration at the acceleration stage. Comprehensively, the fit degree is relatively low using the OV model simulation of car-following Processes 1 and 2.

3.2. GF Model. Helbing and Tilch [9] calibrated the OV model with the empirical data and found that unrealistically high acceleration and deceleration appear in the OV model. To obtain improved results, Helbing and Tilch developed a GF model which is formulated as follows:

$$\begin{aligned} a_n(t) &= \kappa\left(V\left(\Delta x_n(t)\right) - v_n(t)\right) \\ &\quad + \lambda H\left(-\Delta v_n(t)\right)\Delta v_n(t), \end{aligned} \tag{6}$$

where λ is the parameter of the GF model, $\Delta v_n(t) = v_{n-1}(t) - v_n(t)$ is the velocity difference between the nth car and its leading car $n-1$ at time t, and $v_{n-1}(t)$ and $v_n(t)$ correspond to the velocities of the $n-1$th and nth cars, and $H(\cdot)$ is the Heaviside function.

Helbing et al. [9] calibrated the parameters of the GF model by using the car-following data of the experimental site. Similar to the OV model, the calibration data are not the measured data at the signalised intersection. Therefore, the GF model is recalibrated by using the measured car-following process data at signalised intersections. Equation (3) is selected as the optimisation criterion, and the ABC algorithm is used to calibrate the model. The number of employed, onlooker, and scout bees is set to 100, 100, and 1, respectively, and the maximum number of stagnation and the number of iterations in the ABC algorithm are set to 1900 and 3000, correspondingly. The same resulting parameters are obtained consistently through repeated analysis of the experiment. Moreover, the algorithm converges to these resulting parameters, and the number of first ABC iterations of the result is at most 2000 times. Thus, the algorithm has converged to the global optimal solution. The resulting parameters of the GF model are $\kappa = 0.11$, $v_1 = 10.51$, $v_2 = 10.38$, $c_1 = 2.13$, $c_2 = 11.01$, and $\lambda = 1.26$.

We selected two complete car-following processes, as displayed in Table 1, to verify the adaptability of the calibrated GF model to the car-following trajectory at the signal intersection. In Table 1, the first point data of the two process data are used as the initial state of the simulation. Then, the complete simulation of the car-following process can be obtained on the basis of the evolution of the model. The simulation results are presented in Figures 5 and 6.

Figure 5(a) exhibits the simulation analysis of the acceleration/deceleration of the GF model in car-following Process 1. This figure shows that the deceleration is faster than the measured data at the early deceleration stage, but the subsequent deceleration stage is slower than the measured data. The acceleration simulation of the GF model is smaller in the acceleration stage than in the measured data. Figure 5(b) displays the simulation analysis of the velocity of the GF model in car-following Process 1. This figure shows that the velocity simulation of the GF model is less than the measured data at the early deceleration and greater than the measured data at the subsequent deceleration stage, similar to the OV model. Figure 5(c) presents the simulation analysis of the distance headway of the GF model in car-following Process 1. This figure shows that the distance headway of the entire deceleration stage is greater than the measured data given the significant deceleration at the early deceleration stage, and the distance headway gradually reduces at the subsequent deceleration stage considering the slow deceleration. Moreover, the distance headway simulation of the GF model at the acceleration stage is close to the measured data. The comprehensive analyses of Figures 5(a), 5(b), and 5(c) show the same results as those obtained through the simulation analysis of acceleration/deceleration, velocity, and distance headway. The GF model simulation of car-following Process 1 has the problem of a significant deceleration in the early deceleration stage and the minimal deceleration at the subsequent deceleration stage. Moreover, the simulation results of the GF model at the acceleration stage are better than the OV model, thereby ensuring that the following car avoids the risk of a rear-end collision. The simulation of car-following Process 1 shows that the GF model is better than the OV model, but the fit degree remains relatively low between the simulation and the measured trajectories when the GF model simulates car-following Process 1.

Figure 6(a) illustrates the simulation analysis of the acceleration/deceleration of the GF model in car-following Process 2. This figure presents that the deceleration is slower than the measured data in the early deceleration stage, and the deceleration is greater than the measured data at the subsequent deceleration stage. The problem of the GF model simulation of car-following Process 2 at the acceleration stage is consistent with that of the OV model. The simulation result shows a slower and insufficient acceleration over the measured data. Figure 6(b) depicts the simulation analysis of the velocity of the GF model in car-following Process 2. This figure shows that the simulation velocity is greater than the measured data at the deceleration stage, and the simulation velocity of the GF model at the acceleration stage is smaller than the measured data. Figure 6(c) demonstrates the simulation analysis of the distance headway of the GF model in car-following Process 2. This figure shows that the distance headway of the following car is close to 5 m during the entire idling stage given the minimal deceleration at the deceleration stage, thereby resulting in the risk of a rear-end collision of the following car. Moreover, the distance headway of the GF model at the acceleration stage is greater than the measured data given the minimal acceleration. The comprehensive analyses of Figures 6(a), 6(b), and 6(c) show the same results as those obtained through the simulation analysis of acceleration/deceleration, velocity, and distance headway. The GF model simulation of car-following Process 2 has a problem similar to the OV model. The deceleration of the GF model simulation process is smaller than the measured data at the deceleration stage, thereby causing the distance headway of the following car to be close to 5 m at the idling stage. The GF model shows a slow and insufficient acceleration over the measured data at the acceleration stage. Therefore, the fit degree remains relatively low between the simulation and the measured trajectories when the OV model simulates car-following Process 2.

The results of the simulation analysis of car-following Processes 1 and 2 by the GF model show that the GF model simulation of the gather and dissipation vehicles has the same problem as the OV model considering the minimal deceleration at the deceleration stage, thereby resulting in the risk of a rear-end collision of the following car. Moreover, the GF model shows a slow and insufficient acceleration over the measured data at the acceleration stage. Comprehensively, the fit degree remains relatively low by using the GF model to simulate car-following Processes 1 and 2.

3.3. FVD Model. Jiang et al. [10] proposed the FVD model by considering the negative and positive velocity differences to avoid an unrealistic acceleration. This model can explain the instance; that is, if the leading car is fast, then the car will not stop, although its headway is smaller than the safe distance. The model can be formulated as follows:

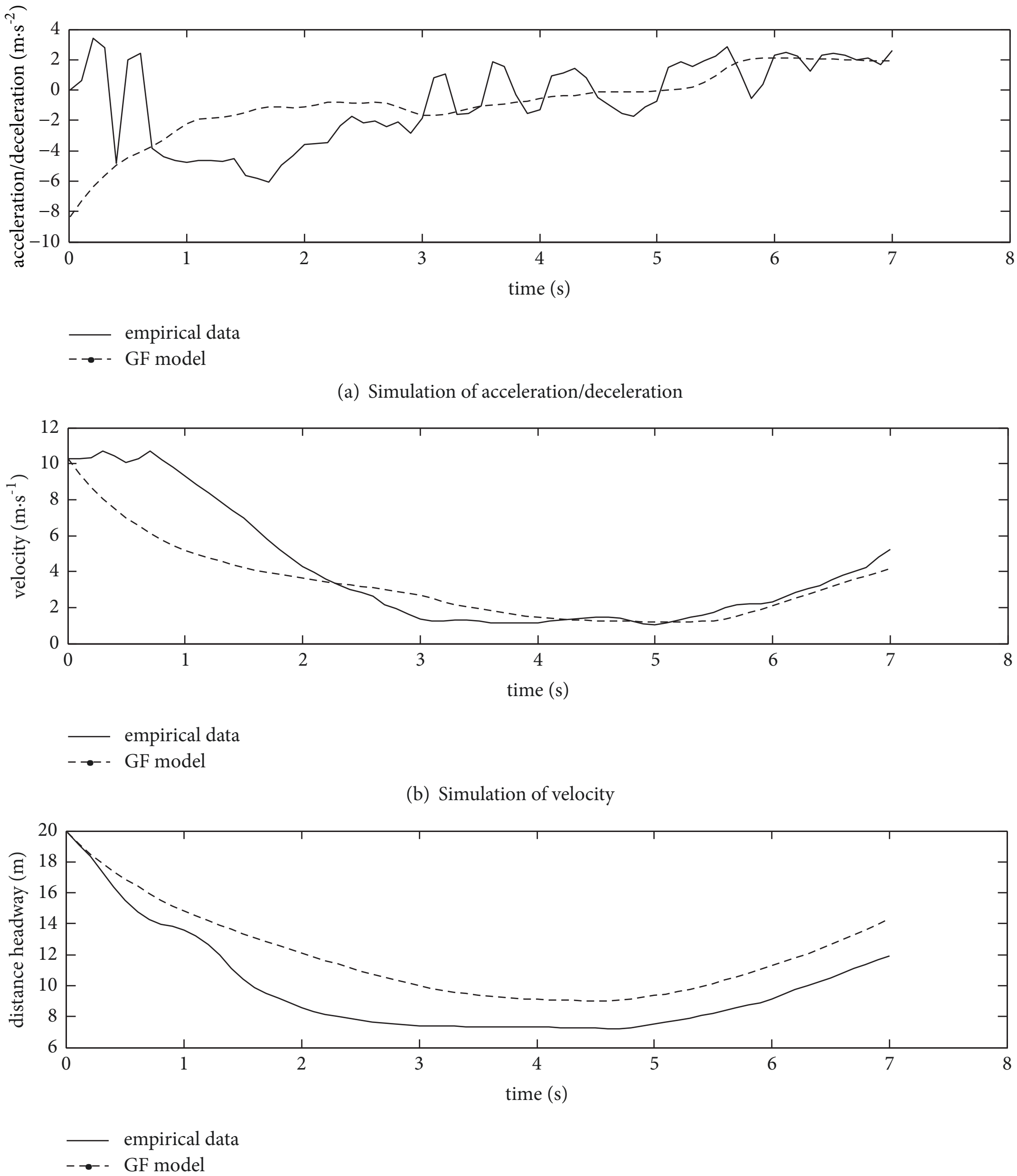

(a) Simulation of acceleration/deceleration

(b) Simulation of velocity

(c) Simulation of distance headway

Figure 5: GF model simulations of car-following Process 1.

$$a_n(t) = \kappa\left(V\left(\Delta x_n(t)\right) - v_n(t)\right) + \lambda \Delta v_n(t), \quad (7)$$

where λ is the parameter of the FVD model.

Similarly, the FVD model is recalibrated by using the measured car-following process data at signalised intersections. Equation (3) is selected as the optimisation criterion, and the ABC algorithm is used to calibrate the model. The number of employed, onlooker, and scout bees is set to 100, 100, and 1, respectively, and the maximum number of stagnation and the number of iterations in the ABC algorithm are set to 1900 and 3000, correspondingly. The same resulting parameters are obtained consistently through a repeated analysis of the experiment. Moreover, the algorithm converges to these resulting parameters, and the number of the first ABC iterations of the result is at most 2000 times. Thus, the algorithm has converged to the global optimal solution. The resulting parameters of the FVD model are $\kappa = 1.93$, $v_1 = 2.49$, $v_2 = 2.45$, $c_1 = 19.69$, $c_2 = 98.14$, and $\lambda = 0.63$.

We selected two complete car-following processes in Table 1 to test the FVD model to verify the adaptability of the calibrated FVD model to the car-following trajectory at the signal intersection. The first point data of the two process data are used as the initial state of the simulation. The complete simulation of the car-following process can then be obtained on the basis of the evolution of the model. The simulation results are demonstrated in Figures 7 and 8.

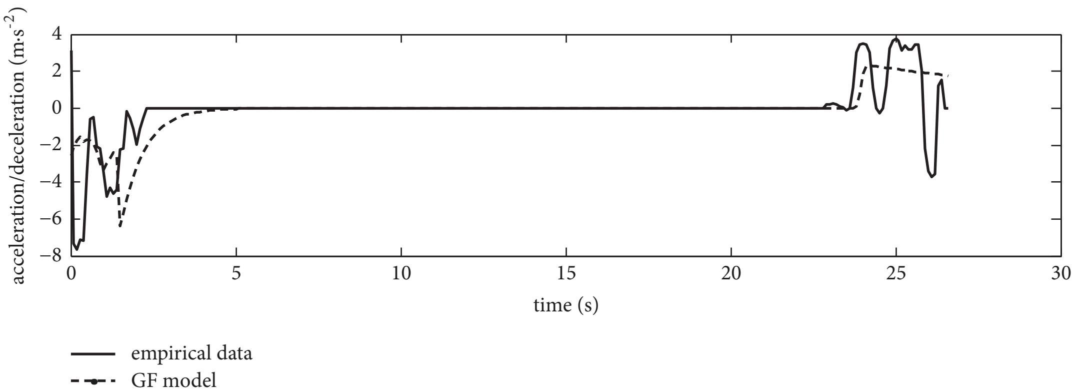

(a) Simulation of acceleration/deceleration

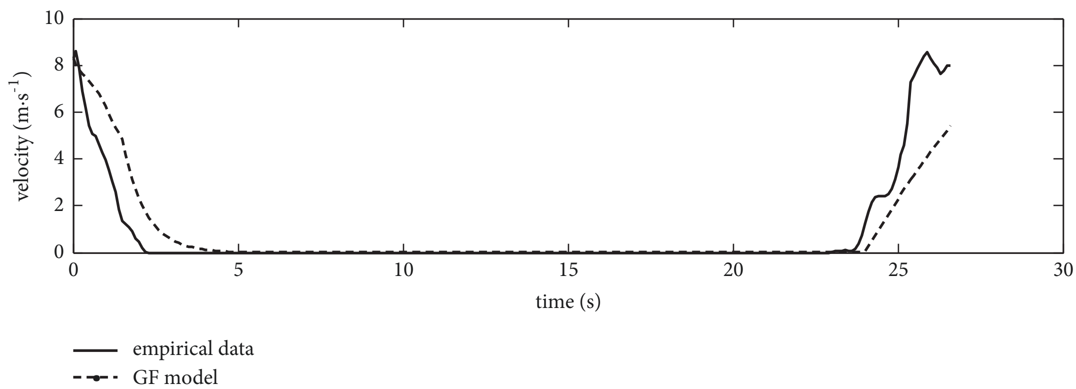

(b) Simulation of velocity

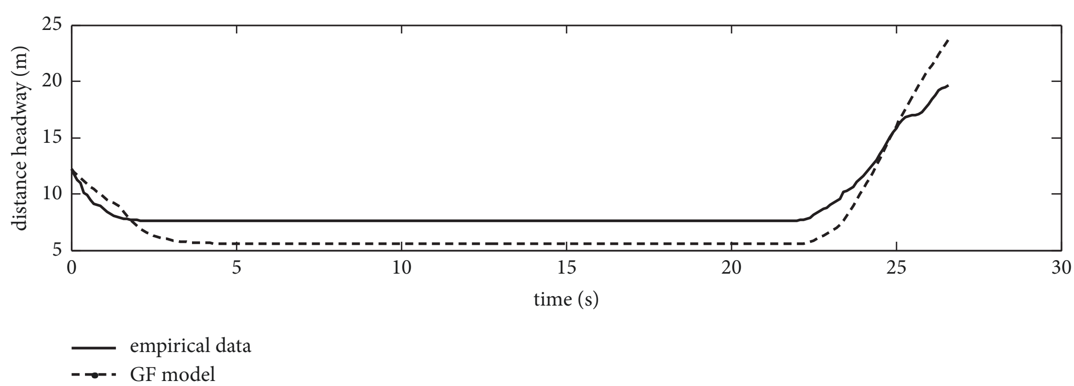

(c) Simulation of distance headway

FIGURE 6: GF model simulations of car-following Process 2.

Figures 7(a), 7(b), and 7(c) exhibit the simulation analyses of the acceleration/deceleration, velocity, and distance headway of the FVD model in car-following Process 1, respectively. Figure 7 displays that the FVD model simulation of car-following Process 1 has the same problem as the OV and GF models. The deceleration of the FVD model is faster than the measured data at the early deceleration stage, but the subsequent deceleration stage is slower than the measured data. Moreover, the simulation results of the FVD model indicate a significant acceleration at the early acceleration stage and avoid an acceleration delay, but the simulation of the entire acceleration process is insufficiently smooth. Overall, the simulation results of the FVD model avoid the risk of a rear-end collision which exists in the OV model. Simultaneously, the problem of acceleration insufficiency in the OV and GF models is solved, but the fit degree remains relatively low between the simulation and measured trajectories when the FVD model is used to simulate car-following Process 1.

Figures 8(a), 8(b), and 8(c) plot the simulation analyses of the acceleration/deceleration, velocity, and distance headway of the FVD model in car-following Process 2, correspondingly. Figure 8 presents that the fit degree of the FVD model simulation in car-following Process 2 at the deceleration process is unfavourable. The deceleration of the FVD model is slower than the measured data at the

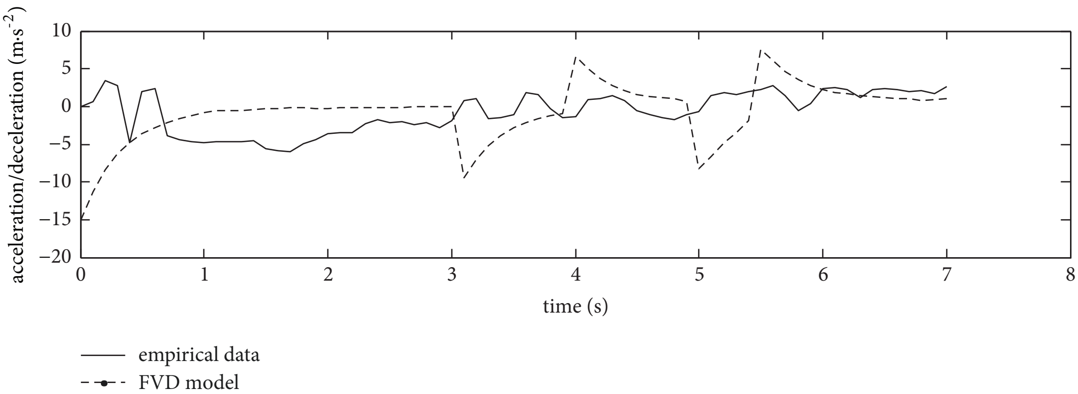

(a) Simulation of acceleration/deceleration

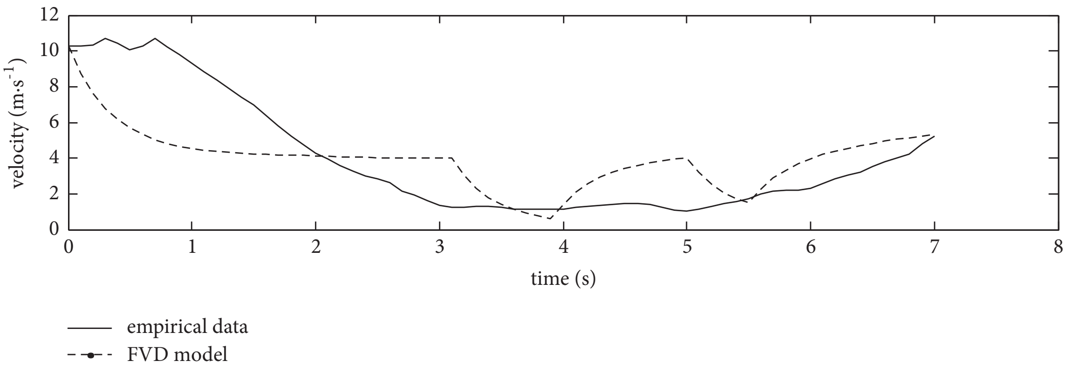

(b) Simulation of velocity

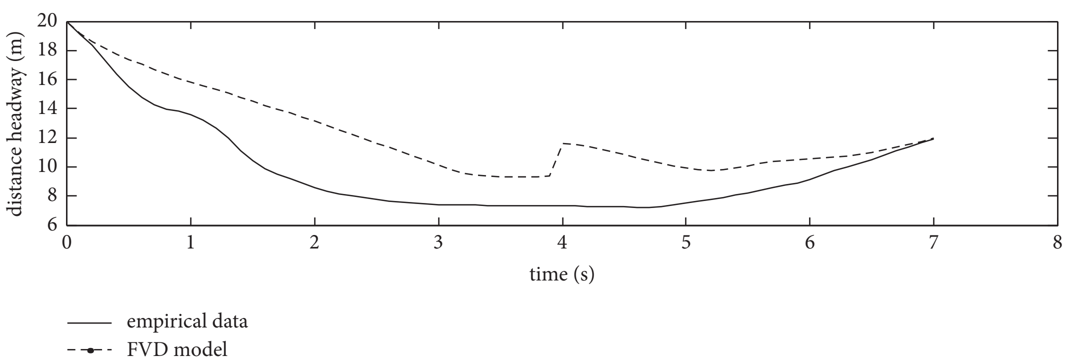

(c) Simulation of distance headway

Figure 7: FVD model simulation of car-following Process 1.

entire deceleration process given the phenomenon of large deceleration at the early deceleration stage, thereby causing the distance headway to become larger than the measured data at the idling stage. The simulation of the FVD model at the acceleration stage avoids the problem of acceleration delay. The acceleration is significant at the early acceleration stage, but the FVD model demonstrates a slow and insufficient acceleration over the measured data at the subsequent acceleration stage, thereby resulting in a deviation between the simulation trajectory and the measured data. Overall, the simulation results of the FVD model avoid the risk of a rear-end collision which exists in the OV model. Simultaneously, the problem of acceleration insufficiency in the OV and GF models at the early acceleration stage is solved. However, the FVD model still has insufficient acceleration at the acceleration stage, and the fit degree remains relatively low between the simulation and the measured trajectories when the FVD model is used to simulate car-following Process 2.

The simulation analysis results of car-following Processes 1 and 2 by the FVD model show that the FVD model has several advantages over the OV model and the GF model, thereby avoiding the risk of a rear-end collision. Moreover, the problem of slow and insufficient acceleration at the early acceleration is solved. However, slow deceleration and insufficient acceleration still occur at the subsequent deceleration and acceleration stage. Comprehensively, the fit degree remains relatively low when the FVD model is used to simulate car-following Processes 1 and 2.

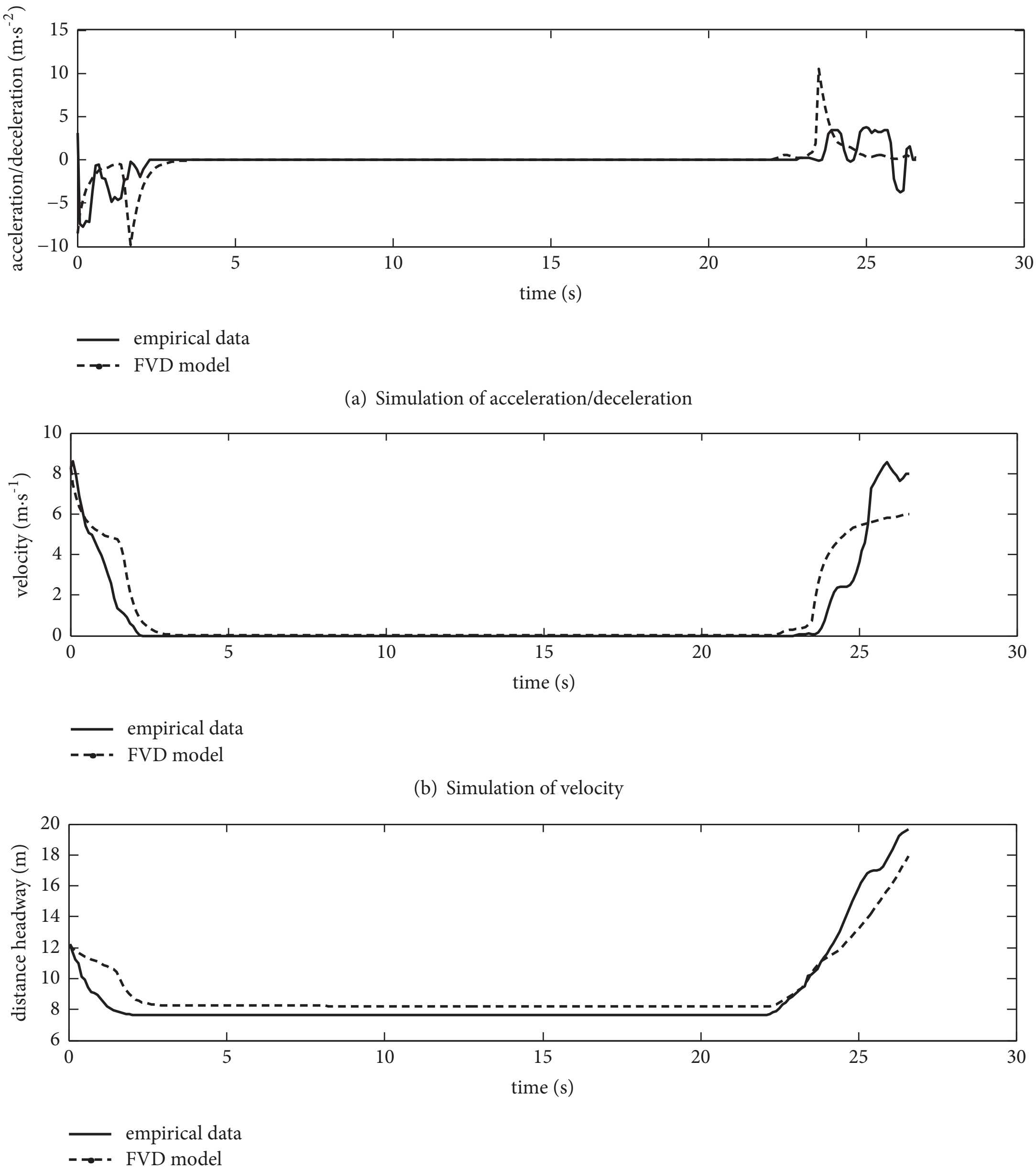

(a) Simulation of acceleration/deceleration

(b) Simulation of velocity

(c) Simulation of distance headway

Figure 8: FVD model simulations of car-following Process 2.

3.4. Other Models. The exploration of an urban signal intersection is important in traffic flow research because it can provide a theoretical basis for intersection signal timing. To describe car-following behaviour at signalised intersection, literature [46–49] proposed various extended car-following models on the basis of the FVD model under the analysis of measured data; literature [51] also proposed an extended car-following model based on the General Motor car-following model. Literature [46] proposed an extended car-following model considering multiple leading cars' acceleration that adapts to vehicle automation and safety early warning systems; literature [47] proposed an improved car-following model considering the velocity difference of an immediately ahead car; literature [48, 49] suggested essentially the same type of car-following model that improved the car-following model considering headway changes with memory on a single lane. Therefore, the car-following models proposed in literature [47, 49] are selected as comparative models, considering the comparability of the improved model proposed in this study. The car-following models proposed in literature [47, 49] can be expressed as follows, respectively.

$$\begin{aligned} a_n(t) &= \kappa\left(V\left(\Delta x_n(t)\right) - v_n(t)\right) + \lambda \Delta v_n(t) \\ &\quad + \gamma\left(v_{n-1}(t) - v_{n-1}(t-1)\right), \end{aligned} \tag{8}$$

$$\begin{aligned} a_n(t) &= \kappa\left(V\left(\Delta x_n(t)\right) - v_n(t)\right) + \lambda \Delta v_n(t) \\ &\quad + \gamma\left(\Delta x_n(t) - \Delta x_n(t-1)\right), \end{aligned} \tag{9}$$

In (8) and (9), $v_{n-1}(t) - v_{n-1}(t-1)$ is velocity difference of the immediately leading car and $\Delta x_n(t) - \Delta x_n(t-1)$ is the headway changes with memory between the nth car and its leading car $n-1$ at time t; γ denotes the sensitivity parameter and the other parameters remain constant.

In the previous analysis, the problems and causes of OV, GF, and FVD model to simulate a microscopic car-following behaviour at signalised intersections are illustrated; it is necessary to propose an extended car-following model to overcome the defects of the OV, GF, and FVD models in simulating the car-following process at signalised intersections. The car-following models proposed in literature [47, 49] are selected as comparative models to illustrate the effectiveness of the improved model. Therefore, these two models need to be recalibrated using the measured car-following data at signalised intersection. Similarly, (3) is selected as the optimisation criterion, and the ABC algorithm is used to calibrate the model. The number of employed, onlooker, and scout bees is set to 100, 100, and 1, respectively, and the maximum number of stagnation and the number of iterations in the ABC algorithm are set to 2200 and 3000, correspondingly. Thus, the algorithm has converged to the global optimal solution. The resulting parameters of the car-following model proposed in literature [47] are $\kappa = 0.48$, $v_1 = 3.21$, $v_2 = -3.15$, $c_1 = -13.58$, $c_2 = -74.57$, $\lambda = 0.58$, and $\gamma = 0.08$ and those of the car-following model proposed in literature [49] are $\kappa = 0.37$, $v_1 = 3.01$, $v_2 = 2.57$, $c_1 = 14.60$, $c_2 = 80.21$, $\lambda = 0.59$, and $\gamma = 0.14$. Notably, the results obtained in this study are not the same as those obtained in literature [47, 49] because of the different car-following data sources. In addition, these two models are selected as comparative models to illustrate the effectiveness of the improved model in the subsequent sections. Therefore, the car-following processes shown in Table 1 will not be used in analysing the two car-following models.

4. Extended Car-Following Model

In Section 3, the OV, GF, and FVD models are used to simulate car-following Processes 1 and 2. The experimental analysis results show that the three models are ineffective for simulating car-following Processes 1 and 2. In the OV, GF, and FVD models, the influence of distance headway on the driving behaviour is insufficiently considered when the vehicles gather at the signalised intersection. In literature [46, 51], actual data were collected through the grey correlation analysis method to obtain a conclusion that the leading vehicle acceleration evidently influences the following vehicle acceleration. In an actual traffic situation, drivers focus on the effect of distance headway while the vehicles gather at signalised intersections. The deceleration amplitude is minimal when the distance headway is large, but the deceleration amplitude increases when the distance headway is small. However, the drivers focus on the acceleration of the front vehicle when the vehicle is dissipated. Therefore, an extended FVD (EFVD) model is proposed to improve the fit degree of the car-following model to simulate the car-following trajectory at signalised intersections. The EFVD model can be formulated as follows:

$$\begin{aligned} a_n(t) &= \kappa\left(V\left(\Delta x_n(t)\right) - v_n(t)\right) + \lambda \Delta v_n(t) \\ &\quad + \mu_1 H\left(-\Delta v_n(t)\right)\left(\Delta x_n(t) - \mu_2\right) \\ &\quad + \mu_3 H\left(\Delta v_n(t)\right) a_{n-1}(t), \end{aligned} \tag{10}$$

where $a_{n-1}(t)$ is the acceleration/deceleration of the $n-1$th car at time t, u_1 is the sensitivity parameter of the distance headway when the vehicles gather, and u_2 is the safe driving distance headway of the driver's deceleration that is different from the parking distance headway. The driver focuses on a minimal deceleration to decelerate when $\Delta x_n(t) \geq u_2$, and if $\Delta x_n(t) < u_2$, then the driver will focus on a large deceleration to decelerate. u_3 is the sensitivity parameter of the acceleration/deceleration of the $n-1$th car. u_1, u_2, and u_3 must be calibrated, and the other parameters remain constant.

The EFVD model is calibrated by using the measured car-following data at signalised intersections. Equation (3) is selected as the optimisation criterion, and the ABC algorithm is used to calibrate the model. The number of employed, onlooker, and scout bees is set to 100, 100, and 1, respectively, and the maximum number of stagnation and the number of iterations in the ABC algorithm are set to 2500 and 3000, correspondingly. The same resulting parameters are obtained every time through repeated analysis of the experiment. Moreover, the algorithm converges to these resulting parameters, and the number of the first ABC iterations of the result is at most 2000 times. Thus, the algorithm has converged to the global optimal solution. The resulting parameters of the FVD model are $\kappa = 0.31$, $v_1 = 5.71$, $v_2 = 5.65$, $c_1 = 6.76$, $c_2 = 67.01$, $\lambda = 0.68$, $\mu_1 = 0.44$, $\mu_2 = 7.27$, and $\mu_3 = 0.31$.

We selected two complete car-following processes, as listed in Table 1, to verify the adaptability of the calibrated EFVD model to the car-following trajectory at the signal intersection and test the EFVD model. The first point data of the two car-following process data are used as the initial state of the simulation. The complete simulation of the car-following process can then be obtained on the basis of the evolution of the model. The simulation results are presented in Figures 9 and 10.

Figures 9(a), 9(b), and 9(c) plot the simulation analyses of the acceleration/deceleration, velocity, and distance headway, respectively, of the EFVD model to car-following Process 1, correspondingly. Figure 9 illustrates that the deceleration of the EFVD model is faster than the measured data at the entire deceleration stage, and the simulation results of the EFVD model at the acceleration stage avoid the problem of acceleration delay and insufficient acceleration. Overall, the EFVD model solves the problem of deceleration rapidly at the early deceleration stage. Moreover, the deceleration is slow at the subsequent deceleration stage in the OV, GF, and FVD models, thereby avoiding the risk of a rear-end collision in the OV model. Simultaneously, the proposed method solves the problem of the insufficient acceleration of the OV and GF models and the unsmoothed acceleration fitting of the FVD model. The EFVD simulation results of car-following Process 1 show a certain improvement over the OV, GF, and FVD models.

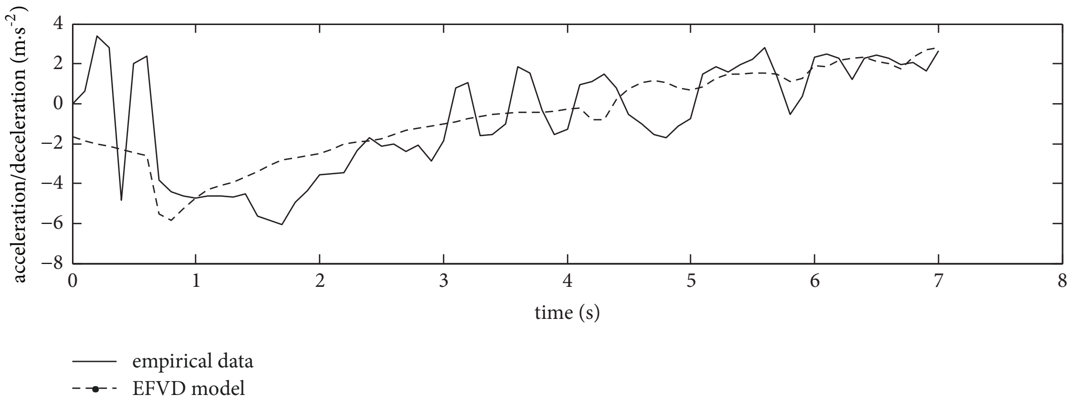

(a) Simulation of acceleration/deceleration

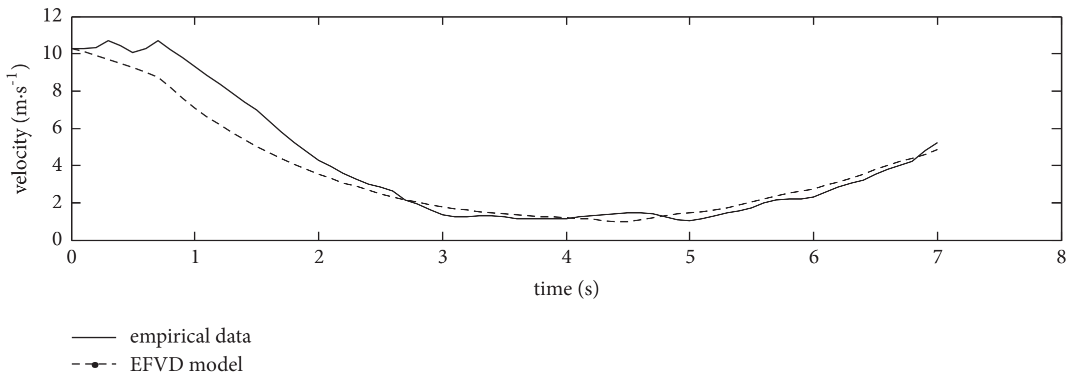

(b) Simulation of velocity

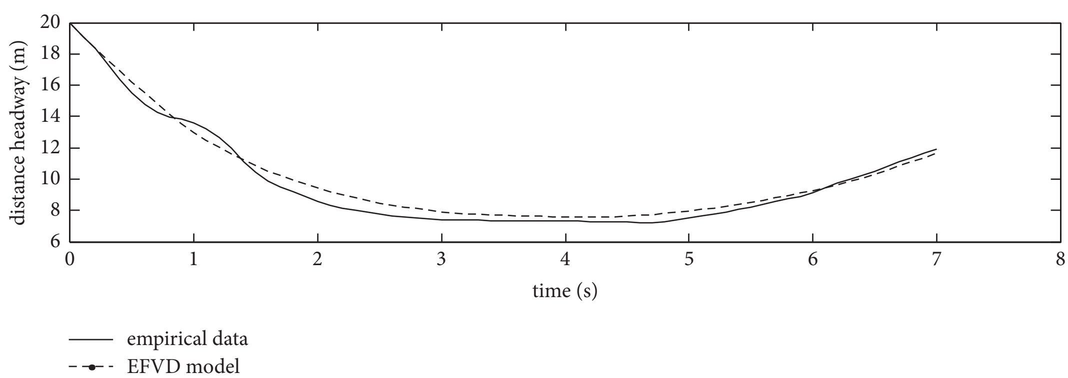

(c) Simulation of distance headway

Figure 9: EFVD model simulations of car-following Process 1.

Figures 10(a), 10(b), and 10(c) plot the simulation analyses of the acceleration/deceleration, velocity, and distance headway of the EFVD model in car-following Process 2, respectively. Figure 10 depicts that the deceleration of the EFVD model is slower than the measured data at the entire deceleration stage, but the distance headway at the idling stage is close to the measured data. The simulation of the EFVD model has a problem of advance acceleration at the acceleration stage but avoids the problem of insufficient acceleration. For car-following Process 2, the EFVD model shows slow deceleration but avoids the risk of a rear-end collision. The proposed model also solves the problem of insufficient acceleration. The EFVD simulation results of car-following Process 2 show a certain improvement over the OV, GF, and FVD models.

The simulation analysis results of car-following Processes 1 and 2 by the EFVD model show that the proposed method can eliminate the rapid deceleration at the early deceleration stage and slow deceleration at the subsequent deceleration stage. The fit degree of car-following Processes 1 and 2 are better in the proposed method than in the OV, GF, and FVD models. However, several problems, such as faster deceleration than the measured data in car-following Process 1 and slower deceleration than the measured data in car-following Process 2, remain. Moreover, the EFVD model simulation of car-following Process 2 has a problem of

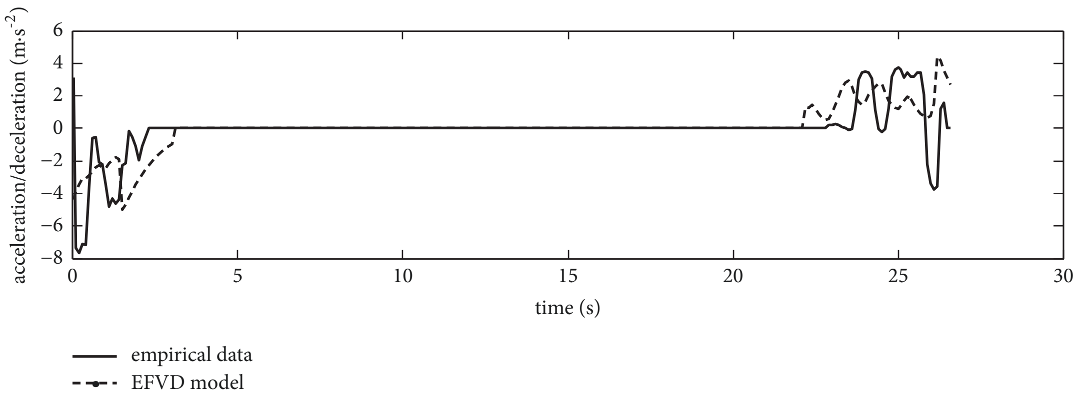

(a) Simulation of acceleration/deceleration

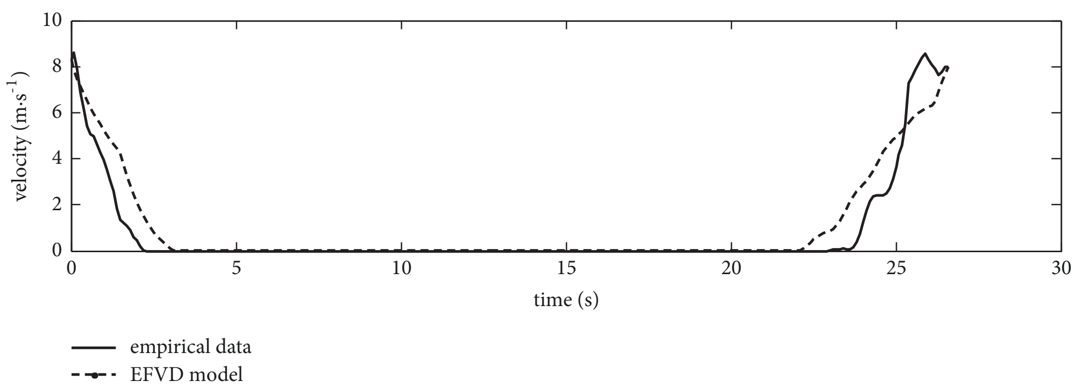

(b) Simulation of velocity

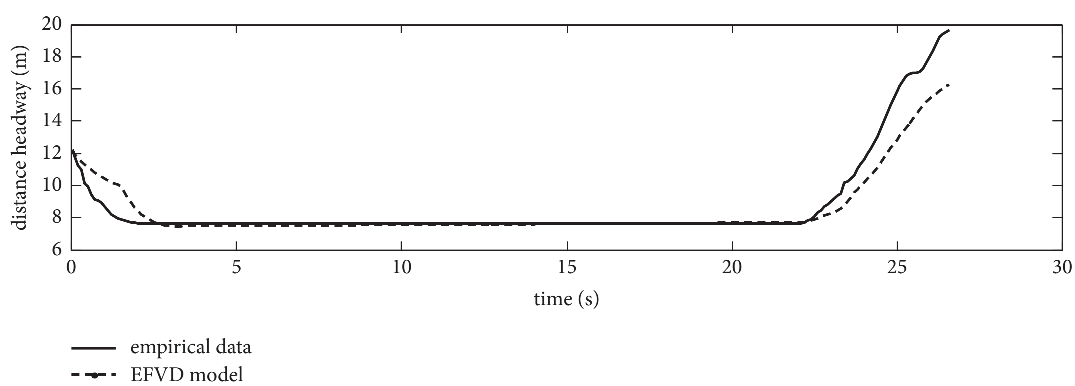

(c) Simulation of distance headway

Figure 10: EFVD model simulations of car-following Process 2.

advance acceleration. The EFVD model is more effective in simulating car-following Processes 1 and 2 than the OV, GF, and FOV models. Similarly, the EFVD model considers the influence of distance headway at the deceleration stage. The model can avoid the problem of early deceleration when the distance headway is large, whereas this model can induce a large deceleration and avoid the risk of a rear-end collision when the distance headway is small. Simultaneously, the problem of low fit degree at the deceleration stage in the OV, GF, and FVD models is solved. The proposed model considers the influence of the acceleration of the leading car at the acceleration stage, although the proposed model causes the problem of advance acceleration. However, the EFVD model solves the problem of acceleration insufficiency and slower acceleration at the late acceleration stage of the FVD model than the OV and GF models.

5. Comparative Analysis

In Section 3, we verified the problems of the OV, GF, and FVD models in fitting the actual car-following behaviour at the signal intersection through the two typical car-following processes. The analysis of its causes indicates that the OV, GF, and FVD models do not consider the car-following distance headway when the vehicle decelerates. Simultaneously, the OV, GF, and FVD models also do not consider the acceleration of the leading vehicle when the vehicle accelerates. The two factors lower the fitting degree of the OV, GF, and FVD models when fitting the actual car-following behaviour at signalised intersections. On the basis of this analysis, we further proposed the EFVD model in Section 4 based on the FVD model. Then, the EFVD model is verified on the basis of the two typical car-following processes. The experimental simulation shows that the EFVD model can solve the problems in the OV, GF, and FVD models. We used three models in this section for comparative analysis to fully demonstrate the superiority of the EFVD model. In this study, we firstly analysed the problems of the OV, GF, and FVD models in fitting the actual car-following behaviour at the signal intersection. Then, we proposed the EFVD model. Thus, we compared the EFVD model with the FVD model, which is better than the OV and GF models, through car-following Processes 1 and 2. The parameters of the FVD and EFVD models are constant, and the comparative results are plotted in Figures 11 and 12, respectively.

Figures 11 and 12 display that the EFVD model is better than the FVD model in simulating car-following Processes 1 and 2. To accurately explain the improvement effect of the EFVD model, (11) is selected as the evaluation criterion to measure the fitting effect of the EFVD and FVD models. Equation (9) can be formulated as follows:

$$PAD = \frac{AD^A - AD^B}{AD^B} \quad (11)$$

where PAD is the prior percentage of the fitting precision of A model to B model when $PAD < 0$. A small PAD represents an improved fitting effect of A model relative to B model while representing a degraded fitting effect of the A model relative to the B model. AD^A and AD^B denote the fitting deviation of certain car-following data using A and B models, respectively, as follows:

$$AD = \left|(0.5v + 0.5\Delta x) - \left(0.5\hat{v} + 0.5\widehat{\Delta x}\right)\right|, \quad (12)$$

where Δx is the calculated distance headway of the car-following model, $\Delta\hat{x}$ is the measured distance headway, v is the calculated velocity of the car-following model, and $\hat{v}$ is the measured velocity.

The calculated results of the fitting deviation of car-following data shown in Table 1 are summarised in Table 2. Table 2 lists the three car-following data for the fitting deviation that is larger in the EFVD model than in the FVD model when simulating car-following Process 1. The 12 other types of car-following data have better fitting results than the FVD model with a minimum improvement of −65.10%. In comparison with the FVD model, the fitting effect of 80% car-following data is improved in car-following Process 1 of the EFVD model simulation. Car-following Process 2 has six car-following data at the early acceleration stage for the fitting deviation that is larger in the EFVD model than in the FVD model. The 48 other car-following data have better fitting results than the FVD model. In comparison with the FVD model, the fitting effect of 88.89% car-following data is improved in car-following Process 2 of the EFVD model simulation. However, the verification analysis is only for the two car-following processes shown in Table 1. Thus, we tested the EFVD model by using the 32 other complete car-following processes, which included 922 isolated point data. In the follow-up comparison process, we abbreviated the FVD model as Model 1. Simultaneously, the car-following models proposed in literature [47, 49] were selected as comparative models and abbreviated as Models 2 and 3, respectively, considering the comparability of the EFVD model proposed in this study. In the testing process, each group of test samples was placed in the model, and the deviation between the output of the model and the measured data was calculated using (12). Then, (11) was selected as the evaluation criterion for the EFVD model compared with Models 1, 2, and 3.

Models 1, 2, and 3 were used to compare and analyse the results, as presented in Figure 13. The graph shows only the comparison results of all data points with starting data of 1 and a gap of 4 to clarify Figure 13. The isolated point used in the EFVD model compared with Models 1, 2, and 3 is only 602 because of the influence of $v_n(t-1)$ and $\Delta x_n(t-1)$ in Models 2 and 3, respectively. Figure 13 illustrates that the PAD value is less than 0 for most of the isolated points when comparing the EFVD with Models 1, 2, and 3. The results show that the fitting degree of the EFVD model for the 602 isolated point data is better than that of Models 1, 2, and 3 for most of the isolated points. However, the fitting degree of partially isolated points in the EFVD model is inferior to Models 1, 2, and 3. According to the statistics of the simulation results, the fitting degree of the EFVD model has 60, 140, and 134 isolated points, which indicates that this model is worse than Models 1, 2, and 3, respectively. Overall, the fitting effect of the EFVD model remains better than that of Models 1, 2, and 3. Fitting effects of 90.03%, 76.74%, and 77.74% isolated points are improved when the EFVD model is compared with Models 1, 2, and 3, respectively. In literature [53], a significant shortage in the comparative testing of the car-following models based on isolated point data was emphasised in calibrating the parameters of the car-following model, and a comprehensive testing of the entire car-following process was lacking, thereby resulting in inaccurate test results. In literature [53], the authors also highlighted that the test of the car-following model should be based on the entire car-following process. Thus, the EFVD model was retested on the basis of the entire car-following process; that is, the first set of data for each car-following process and all subsequent model inputs were based on the computational evolution of the model itself. Furthermore, (12) was used to calculate the deviation of each set of data for each process. The fitting deviation of each car-following process is then calculated using the following:

$$ED = \frac{1}{n}\sum_{i=1}^{n} AD_i, \quad (13)$$

where n is the number of isolated points that are included in each of the car-following processes and AD_i is the deviation for each isolated point data. The EFVD model was tested on the basis of the 32 complete car-following processes. Models 1, 2, and 3 were adopted as the comparative model. The ED

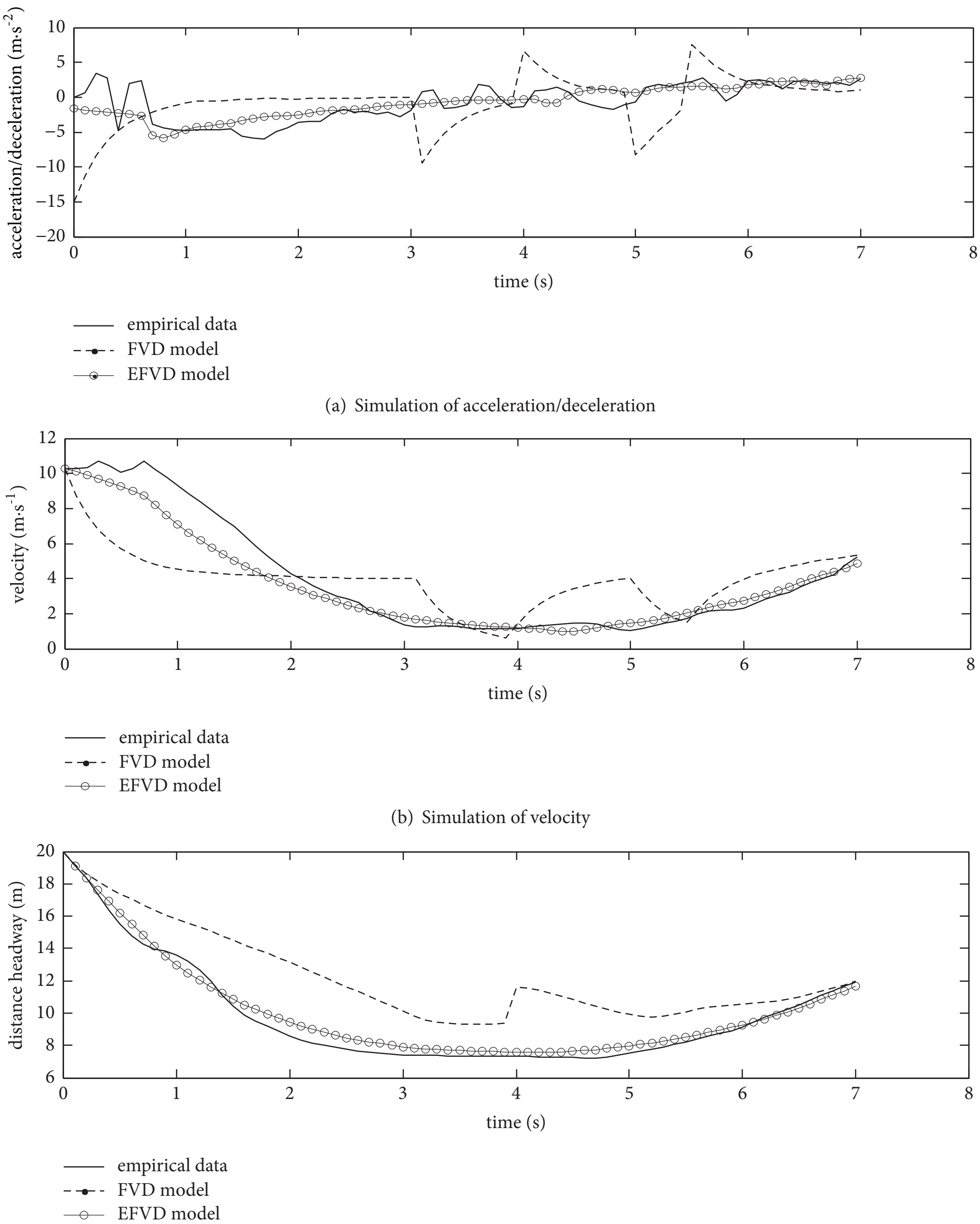

(a) Simulation of acceleration/deceleration

(b) Simulation of velocity

(c) Simulation of distance headway

Figure 11: Simulation comparison of car-following Process 1.

of the different models are presented in Table 3, and the comparative results are summarised in Table 4.

Tables 3 and 4 list six, eight, and nine test car-following processes for the simulation deviation that is larger in the EFVD model than in Models 1, 2, and 3, respectively. The remaining car-following processes indicate that the simulation deviation is better in the EFVD model than in Models 1, 2, and 3, and the improvement of the simulation is evident. According to the statistics of the simulation results, the fitting effect of 90.03%, 76.74%, and 77.74% test car-following processes is improved when the EFVD model is compared with Models 1, 2, and 3, correspondingly. Therefore, the EFVD model from the overall perspective is better than Models 1, 2, and 3 in simulating the car-following process at signalised intersections.

The comprehensive analysis results indicate the EFVD model several advantages over Models 1, 2, and 3, whether the proposed model is tested on the basis of the isolated

Table 2: Fitting deviation of car-following data in Table 1.

Car-following processes	Number of isolated points	*AD* of the FVD model	*AD* of the EFVD model	*PAD* (EFVD model compared with FVD model)
	1	0.00	0.00	0.00%
	2	1.26	0.06	-95.58%
	3	1.26	1.40	11.64%
	4	0.66	0.78	18.20%
	5	2.18	0.05	-97.59%
	6	2.52	0.18	-93.00%
	7	2.69	0.48	-82.13%
1	8	1.08	0.27	-74.81%
	9	0.76	0.18	-76.21%
	10	2.79	0.03	-99.00%
	11	2.66	0.42	-84.24%
	12	0.81	0.28	-65.10%
	13	1.53	0.27	-82.44%
	14	0.90	0.04	-95.19%
	15	0.07	0.10	40.19%

Table 2: Continued.

Car-following processes	Number of isolated points	*AD* of the FVD model	*AD* of the EFVD model	*PAD* (EFVD model compared with FVD model)
2	1	0.00	0.00	0.00%
	2	0.92	1.28	-27.90%
	3	1.71	1.62	-5.28%
	4	3.00	2.48	-17.31%
	5	1.14	1.05	-8.10%
	6	0.55	0.15	-72.29%
	7	0.72	0.45	-38.44%
	8	0.64	0.48	-24.07%
	9	0.62	0.50	-18.14%
	10	0.61	0.50	-17.29%
	11	0.61	0.50	-16.89%
	12	0.60	0.51	-15.57%
	13	0.60	0.50	-16.87%
	14	0.60	0.50	-17.39%
	15	0.60	0.49	-17.51%
	16	0.60	0.49	-17.43%
	17	0.59	0.49	-17.25%
	18	0.59	0.49	-17.02%
	19	0.59	0.49	-16.77%
	20	0.59	0.49	-16.50%
	21	0.59	0.49	-16.22%
	22	0.58	0.50	-14.92%
	23	0.58	0.49	-16.22%
	24	0.58	0.48	-16.73%
	25	0.58	0.48	-16.83%
	26	0.58	0.48	-16.74%
	27	0.57	0.48	-16.55%
	28	0.57	0.48	-16.31%
	29	0.57	0.48	-16.04%
	30	0.57	0.48	-15.76%
	31	0.57	0.48	-15.46%
	32	0.56	0.48	-14.15%
	33	0.56	0.48	-15.44%
	34	0.56	0.47	-15.94%
	35	0.56	0.47	-16.03%
	36	0.56	0.47	-15.93%
	37	0.55	0.47	-15.72%
	38	0.55	0.47	-15.47%
	39	0.55	0.47	-15.18%
	40	0.55	0.47	-14.89%
	41	0.55	0.47	-14.58%
	42	0.54	0.47	-13.66%
	43	0.54	0.46	-14.74%
	44	0.54	0.46	-15.11%
	45	0.54	0.88	63.61%
	46	0.49	0.96	94.77%
	47	0.32	1.00	211.04%
	48	0.64	1.17	83.57%
	49	0.57	0.87	53.46%
	50	0.42	1.53	261.01%
	51	1.53	1.42	-6.86%
	52	2.99	2.23	-25.32%
	53	2.99	2.27	-24.06%
	54	2.25	1.84	-18.30%

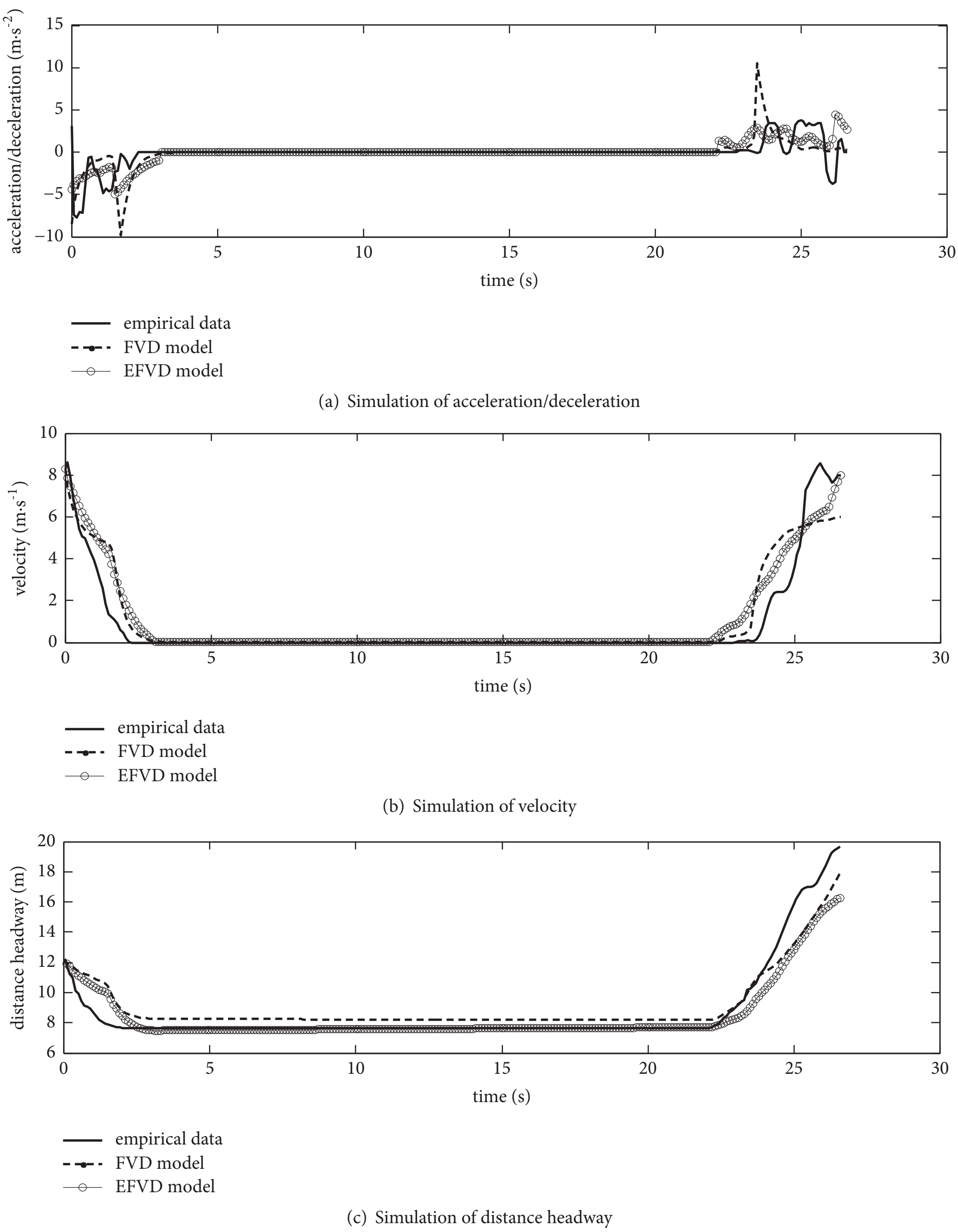

Figure 12: Simulation comparison of car-following Process 2.

point data or the entire car-following process. In combination with the previous analysis, Model 1 ignores the influence of distance headway on the driving behaviour when the vehicles gathered at the signalised intersections and insufficient acceleration occurs at the acceleration stage. Furthermore, we conducted an in-depth analysis of Models 2 and 3. Model 2 was proposed considering the velocity difference of the leading car, and Model 3 was proposed considering the distance headway changes with memory. In comparison with the EFVD model, although Model 2 was proposed based on Model 1 considering the velocity difference of the leading car, the influence of the distance headway on the deceleration behaviour of the drivers was neglected. Model 3 was proposed based on Model 1 considering the distance headway change with memory, but the distance headway at different deceleration stages had a different effect on the deceleration behaviour of the drivers, and the velocity difference of the leading car was also neglected in Model

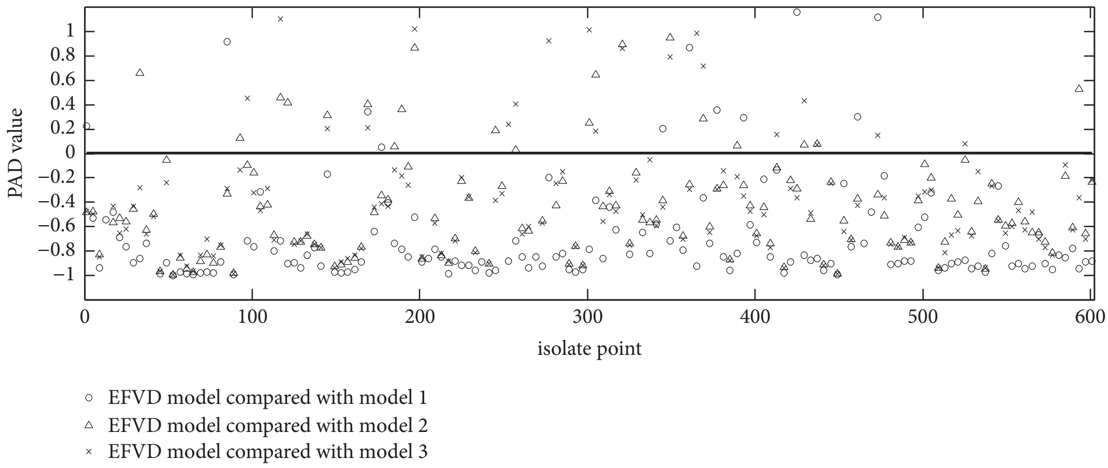

Figure 13: Comparison of the EFVD with Models 1, 2, and 3.

Table 3: *ED* of the different models.

Car-following process	*ED* of the EFVD model	*ED* of Model 1	*ED* of Model 2	*ED* of Model 3
1	0.18	0.74	0.30	0.29
2	0.52	0.45	0.48	0.51
3	0.27	1.32	0.52	0.32
4	0.81	1.81	0.91	0.93
5	0.38	1.15	0.41	0.43
6	0.24	0.71	0.31	0.36
7	0.42	0.50	0.31	0.31
8	0.52	0.92	0.54	0.52
9	0.30	1.54	0.52	0.35
10	0.22	0.42	0.31	0.32
11	0.32	0.57	0.23	0.23
12	0.20	1.06	0.22	0.21
13	0.55	0.45	0.66	0.66
14	0.36	0.61	0.18	0.17
15	0.54	1.06	0.76	0.82
16	0.37	0.29	0.31	0.31
17	0.24	0.40	0.33	0.32
18	0.70	0.83	0.78	0.76
19	0.31	0.76	0.25	0.28
20	0.04	0.64	0.14	0.13
21	0.32	0.98	0.50	0.41
22	0.14	0.24	0.16	0.17
23	0.17	0.44	0.22	0.19
24	0.93	1.70	1.28	1.36
25	0.49	2.02	1.55	1.61
26	0.81	1.68	1.18	1.29
27	0.61	1.44	0.65	0.67
28	0.49	0.27	0.54	0.56
29	0.42	0.40	0.25	0.24
30	0.11	0.94	0.40	0.39
31	0.31	0.66	0.22	0.23
32	0.50	0.36	0.63	0.63

Table 4: Analysis of the EFVD compared with Models 1, 2, and 3 on the basis of the car-following process.

Car-following process	(*ED* of the EFVD model– *ED* of Model 1)/*ED* of Model 1	(*ED* of the EFVD model– *ED* of Model 2)/*ED* of Model 2	(*ED* of the EFVD model– *ED* of Model 3)/*ED* of Model 3
1	-74.95%	-37.67%	-36.29%
2	13.82%	6.64%	2.01%
3	-79.81%	-48.52%	-17.10%
4	-55.29%	-10.90%	-13.30%
5	-66.72%	-7.87%	-11.25%
6	-65.69%	-20.66%	-32.48%
7	-16.34%	35.44%	36.70%
8	-43.03%	-2.70%	1.82%
9	-80.28%	-41.18%	-13.43%
10	-48.32%	-29.23%	-32.13%
11	-43.65%	39.08%	41.40%
12	-81.29%	-9.63%	-6.49%
13	20.70%	-16.95%	-17.23%
14	-40.81%	105.85%	115.86%
15	-48.66%	-28.35%	-34.07%
16	29.12%	21.87%	21.34%
17	-39.12%	-27.23%	-25.46%
18	-15.54%	-9.91%	-7.78%
19	-58.82%	23.47%	12.56%
20	-93.75%	-70.83%	-70.07%
21	-67.72%	-37.08%	-23.61%
22	-40.38%	-12.78%	-15.55%
23	-61.74%	-22.40%	-12.21%
24	-45.58%	-27.83%	-31.74%
25	-75.79%	-68.41%	-69.61%
26	-51.94%	-31.81%	-37.16%
27	-57.77%	-7.37%	-9.47%
28	79.26%	-9.79%	-13.19%
29	3.55%	67.01%	73.15%
30	-88.85%	-73.68%	-73.28%
31	-52.98%	42.94%	35.14%
32	39.30%	-20.69%	-20.00%

3. In this study, the improvement of the EFVD model is different from that of Models 2 and 3. We distinguished the vehicles that gather and dissipation based on the velocity of following and leading vehicles. In comparison with Model 2, the EFVD model emphasised the effect of acceleration on car-following behaviour only at the acceleration stage that was different from that of Model 2. In comparison with Model 3, the EFVD model highlighted the influence of headway distance on vehicle deceleration behaviour at different deceleration stages. Moreover, we determined the average safe driving distance headway of the driver's deceleration based on parameter u_2. When the distance headway is greater than u_2, the vehicle will decelerate with a small deceleration. By contrast, when the distance headway is smaller than u_2, the vehicle will decelerate with a large deceleration. This improvement method avoids the risk of a rear-end collision. Comprehensively, the EFVD model distinguishes the vehicles that gather and dissipation based on the velocity of following and leading vehicles. The effects of different factors on the car-following behaviour were considered at different stages. The EFVD model can improve the deficiencies in the OV, GF, and FVD models. However, we still need to explain the worse fitting degree of the EFVD model than Models 1, 2, and 3 in the partially isolated point and car-following process. We analysed the EFVD model and the simulation of the car-following behaviour. The main reasons for the insufficient fitting of the EFVD model were caused by parameters u_2 and $a_{n-1}(t)$ in the EFVD model, and u_2 was the average safe driving distance headway of the driver's deceleration which is decided by numerous car-following processes. In the actual car-following environment, the safe driving distance headway of the driver's deceleration is inconsistent with u_2, given the

influence of the driver's characteristics. When the driver's driving behaviour is aggressive and unsteady, the driver's deceleration safety distance is often less than the parameter u_2. When the driver's driving behaviour is conservative and careful, the driver's deceleration safety distance is often greater than parameter u_2. In these two cases, the EFVD model was insufficient to simulate deceleration behaviour because of the influence of parameter u_2. The EFVD model also considers the effect of $a_{n-1}(t)$ in solving the problem of insufficient acceleration in the FVD model. However, this effect results in the problem of advanced acceleration at the early acceleration stage. The analysis of the experimental simulation indicates that when the car-following process contains more data points, the acceleration data points in the early stage are relatively less, and the fitting degree improvement of the entire car-following process brought by parameter $a_{n-1}(t)$ is better than the fitting degree error caused by the advanced acceleration. Conversely, when the car-following process contains less data points, the acceleration data points in the early stage are relatively more, and the advanced acceleration caused by parameter $a_{n-1}(t)$ has a relatively worse effect on the fitting degree improvement of the entire car-following process. The two factors combined cause the EFVD model to have several defects. Overall, the improvement effect of the EFVD model in most of the test data is evident, although the EFVD model is worse than Models 1, 2, and 3 in the partially isolated point and car-following process.

6. Conclusion

The car-following behaviour at signalised intersections is different from that on the road. The driving behaviour when the vehicle is gathered is also different from the driving behaviour when the vehicle is dissipated. The OV, GF, and FVD models are tested by using two types of car-following processes, namely, incomplete and complete parking, to address the abovementioned problem. The results show that the deceleration of the three models is larger than the measured data at the early stage of deceleration. However, the deceleration is smaller than the measured data at the subsequent deceleration stage. Moreover, the simulation of the car-following behaviour at signalised intersections using the OV and GF models demonstrates the risk of a rear-end collision. The OV and GF models at the acceleration stage have the problem of acceleration insufficiency in the entire acceleration stage, although the FVD model has a significant acceleration in the early acceleration stage. However, the acceleration remains insufficient at the subsequent acceleration stage. We consider the effect of distance headway on the following behaviour when the vehicle is gathered and the effect of the acceleration of the front vehicle on the following behaviour when the vehicle is dissipated to solve the deficiencies of the three models because the driver has different emphases when the vehicle is gathered and when dissipated. Furthermore, we propose the EFVD model on the basis of the FVD model. The experimental analysis confirms that the EFVD model can improve the deficiencies in the OV, GF, and FVD models. Furthermore, the 622 isolated point data of the 32 complete car-following processes are used to test the EFVD model, FVD model, and two other models which are adopted as the comparative model. The results show that the simulation fit is better in the EFVD model than in the FVD model for most of the test data. Thus, the extended model is effective. The EFVD model is more reasonable than the OV, GF, FVD, and two other models for analysing the car-following behaviour at signalised intersections.

However, a certain deficiency is observed in the EFVD model considering the influence of parameters u_2 and $a_{n-1}(t)$, similar to the previous analysis. Thus, improving this model should firstly focus on driver character analysis and dynamic adjustment of the parameter u_2 value in combination with driver's character, and the determination of other parameters should also be combined with the driver's character. Secondly, we should dynamically adjust the coefficient of $a_{n-1}(t)$ in accordance with the velocity of the following vehicle considering the problem of advance acceleration at the early acceleration stage in this model. We can then further improve the fitting degree of the EFVD model for simulating the measured data of the car-following behaviour at signalised intersections. The car-following model summarises the characteristics of many drivers and describes these characteristics mathematically. The simulation results show the average driving behaviour. In the actual driving behaviour, the car-following model cannot fully fit the trajectory of the vehicle given the influence of various conditions. Therefore, we propose various new car-following models that adapt to the automatic driving environment with the rapid development of information and vehicle technologies. In the next stage, we will focus on analysing the influencing factors of the car-following model at signal intersections under the automatic driving environment. We will further improve the traditional car-following model and develop an enhanced car-following model at signalised intersections to adapt to the automatic driving environment.

Data Availability

The data for the simulation analysis used in the present study are derived from the NGSIM programme; the Lankershim Boulevard datasets are freely available for download at the https://www.fhwa.dot.gov/publications/research/operations/its/06135/index.cfm.

Conflicts of Interest

The authors declare that they have no conflicts of interest.

Acknowledgments

The work described in this paper was fully supported by the National Nature Science Foundation of China (no. 61364026). Any opinions, findings, conclusions, or recommendations expressed in this paper do not reflect the views of the Government of the China for the Innovation and Technology Support Program of the Innovation and Technology Fund.

References

[1] M. Brackstone and M. McDonald, "Car-following: a historical review," *Transportation Research Part F: Traffic Psychology and Behaviour*, vol. 2, no. 4, pp. 181–196, 1999.

[2] R. E. Chandler, R. Herman, and E. Montroll, "Traffic dynamics: studies in car following," *Operations Research*, vol. 6, no. 2, pp. 165–184, 1958.

[3] R. Herman, E. W. Montroll, R. B. Potts, and R. W. Rothery, "Traffic dynamics: analysis of stability in car following," *Operations Research*, vol. 7, no. 1, pp. 86–106, 1959.

[4] A. Reuschel, "Fahrzeugbewegungen in der kolonne," vol. 4, no. 3, 1950.

[5] L. A. Pipes, "An operational analysis of traffic dynamics," *Journal of Applied Physics*, vol. 24, pp. 274–281, 1953.

[6] D. C. Gazis, R. Herman, and R. W. Rothery, "Nonlinear follow-the-leader models of traffic flow," *Operations Research*, vol. 9, no. 4, pp. 545–567, 1961.

[7] G. F. Newell, "Nonlinear effects in the dynamics of car following," *Operations Research*, vol. 9, no. 2, pp. 209–229, 1961.

[8] M. Bando, K. Hasebe, A. Nakayama, A. Shibata, and Y. Sugiyama, "Dynamical model of traffic congestion and numerical simulation," *Physical Review E Statistical Physics Plasmas Fluids & Related Interdisciplinary Topics*, vol. 51, no. 2, 1995.

[9] D. Helbing and B. Tilch, "Generalized force model of traffic dynamics," *Physical Review E: Statistical, Nonlinear, and Soft Matter Physics*, vol. 58, no. 1, pp. 133–138, 1998.

[10] R. Jiang, Q. Wu, and Z. Zhu, "Full velocity difference model for a car-following theory," *Physical Review E: Statistical, Nonlinear, and Soft Matter Physics*, vol. 64, part 2, no. 1, 2001.

[11] X. Zhao and Z. Gao, "A new car-following model: full velocity and acceleration difference model," *The European Physical Journal B*, vol. 47, no. 1, pp. 145–150, 2005.

[12] A. K. Gupta and V. K. Katiyar, "Phase transition of traffic states with on-ramp," *Physica A: Statistical Mechanics and Its Applications*, vol. 371, no. 2, pp. 674–682, 2006.

[13] A. K. Gupta and V. K. Katiyar, "A new anisotropic continuum model for traffic flow," *Physica A: Statistical Mechanics and Its Applications*, vol. 368, no. 2, pp. 551–559, 2006.

[14] T. Wang, Z.-Y. Gao, and X.-M. Zhao, "Multiple velocity difference model and its stability analysis," *Acta Physica Sinica*, vol. 55, no. 2, pp. 634–640, 2006.

[15] A. K. Gupta and V. K. Katiyar, "A new multi-class continuum model for traffic flow," *Transportmetrica*, vol. 3, no. 1, pp. 73–85, 2007.

[16] H. X. Ge, R. J. Cheng, and Z. P. Li, "Two velocity difference model for a car following theory," *Physica A Statistical Mechanics & Its Applications*, vol. 387, no. 21, pp. 5239–5245, 2008.

[17] Z. Wen-Xing and J. Lei, "Nonlinear analysis of a synthesized optimal velocity model for traffic flow," *Communications in Theoretical Physics*, vol. 50, no. 2, pp. 505–510, 2008.

[18] H. X. Gong, H. C. Liu, and B.-H. Wang, "An asymmetric full velocity difference car-following model," *Physica A: Statistical Mechanics and Its Applications*, vol. 387, no. 11, pp. 2595–2602, 2008.

[19] G. H. Peng and D. H. Sun, "A dynamical model of car-following with the consideration of the multiple information of preceding cars," *Physics Letters A*, vol. 374, no. 15-16, pp. 1694–1698, 2010.

[20] W. X. Zhu and J. Lei, "Stability and kinku2013antikink soliton solution for total generalized optimal velocity model," *International Journal of Modern Physics C*, vol. 19, no. 9, 2008.

[21] T. Q. Tang, Y. H. Wu, L. Caccetta, and H. J. Huang, "A new car-following model with consideration of roadside memorial," *Physics Letters A*, vol. 375, no. 44, pp. 3845–3850, 2011.

[22] Y. F. Jin, M. Xu, and Z. Y. Gao, "KdV and kink-antikink solitons in an extended car-following model," *Journal of Computational and Nonlinear Dynamics*, vol. 6, no. 1, pp. 52–63, 2011.

[23] T. Q. Tang, C. Y. Li, Y. H. Wu, and H. J. Huang, "Impact of the honk effect on the stability of traffic flow," *Physica A Statistical Mechanics & Its Applications*, vol. 390, no. 20, pp. 3362–3368, 2011.

[24] Y. Li, D. Sun, W. Liu et al., "Modeling and simulation for microscopic traffic flow based on multiple headway, velocity and acceleration difference," *Nonlinear Dynamics*, vol. 66, no. 1-2, pp. 15–28, 2011.

[25] S. Jin, D.-H. Wang, and X.-R. Yang, "Non-lane-based car-following model with visual angle information," *Transportation Research Record*, no. 2249, pp. 7–14, 2011.

[26] Y. F. Jin and M. Xu, "Bifurcation analysis of the full velocity difference model," *Chinese Physics Letters*, vol. 27, no. 4, pp. 53–55, 2010.

[27] S. Jin, D. H. Wang, Z. Y. Huang, and P. F. Tao, "Visual angle model for car-following theory," *Physica A: Statistical Mechanics & Its Applications*, vol. 390, no. 11, pp. 1931–1940, 2011.

[28] A. K. Gupta and V. K. Katiyar, "Analyses of shock waves and jams in traffic flow," *Journal of Physics A: Mathematical and Theoretical*, vol. 38, no. 19, pp. 4069–4083, 2005.

[29] S. Jin, D. H. Wang, C. Xu, and Z. Y. Huang, "Staggered car-following induced by lateral separation effects in traffic flow," *Physics Letters A*, vol. 376, no. 3, pp. 153–157, 2012.

[30] T. Tang, H. Huang, and H. Shang, "A new pedestrian-following model for aircraft boarding and numerical tests," *Nonlinear Dynamics*, vol. 67, no. 1, pp. 437–443, 2012.

[31] T. Q. Tang, Y. P. Wang, X. B. Yang, and Y. H. Wu, "A new car-following model accounting for varying road condition," *Nonlinear Dynamics*, vol. 70, no. 2, pp. 1397–1405, 2012.

[32] T. Tang, Y. Shi, Y. Wang, and G. Yu, "A bus-following model with an on-line bus station," *Nonlinear Dynamics*, vol. 70, no. 1, pp. 209–215, 2012.

[33] G.-H. Peng and R.-J. Cheng, "A new car-following model with the consideration of anticipation optimal velocity," *Physica A: Statistical Mechanics and Its Applications*, vol. 392, no. 17, pp. 3563–3569, 2013.

[34] A. K. Gupta, "A section approach to a traffic flow model on networks," *International Journal of Modern Physics C*, vol. 24, no. 5, 2013.

[35] A. K. Gupta, S. Sharma, and P. Redhu, "Analyses of lattice traffic flow model on a gradient highway," *Communications in Theoretical Physics*, vol. 62, no. 3, pp. 393–404, 2014.

[36] A. K. Gupta and I. Dhiman, "Analyses of a continuum traffic flow model for a nonlane-based system," *International Journal of Modern Physics C*, vol. 25, no. 10, p. 4, 2014.

[37] A. K. Gupta and P. Redhu, "Analyses of the driver's anticipation effect in a new lattice hydrodynamic traffic flow model with passing," *Nonlinear Dynamics*, vol. 76, no. 2, pp. 1001–1011, 2014.

[38] J. I. Ge and G. Orosz, "Dynamics of connected vehicle systems with delayed acceleration feedback," *Transportation Research Part C: Emerging Technologies*, vol. 46, pp. 46–64, 2014.

[39] T. Tang, W. Shi, H. Shang, and Y. Wang, "A new car-following model with consideration of inter-vehicle communication," *Nonlinear Dynamics*, vol. 76, no. 4, pp. 2017–2023, 2014.

[40] W.-X. Zhu and L.-D. Zhang, "A speed feedback control strategy for car-following model," *Physica A: Statistical Mechanics and Its Applications*, vol. 413, pp. 343–351, 2014.

[41] T. Zhou, D. Sun, Y. Kang, H. Li, and C. Tian, "A new car-following model with consideration of the prevision driving behavior," *Communications in Nonlinear Science and Numerical Simulation*, vol. 19, no. 10, pp. 3820–3826, 2014.

[42] A. K. Gupta and I. Dhiman, "Phase diagram of a continuum traffic flow model with a static bottleneck," *Nonlinear Dynamics*, vol. 79, no. 1, pp. 663–671, 2015.

[43] S. Sharma, "Lattice hydrodynamic modeling of two-lane traffic flow with timid and aggressive driving behavior," *Physica A: Statistical Mechanics and Its Applications*, vol. 421, pp. 401–411, 2015.

[44] M. Sasaki and T. Nagatani, "Transition and saturation of traffic flow controlled by traffic lights," *Physica A: Statistical Mechanics and Its Applications*, vol. 325, no. 3-4, pp. 531–546, 2003.

[45] T. Tang, G. Xu, H.-J. Huang, and Y. Xue, "A traffic flow model considering signal light influence and its numerical simulation," *Acta Physica Sinica*, vol. 57, no. 1, pp. 56–60, 2008.

[46] S. Yu and Z. Shi, "An extended car-following model at signalized intersections," *Physica A: Statistical Mechanics and Its Applications*, vol. 407, pp. 152–159, 2014.

[47] S. Yu, X. Zhao, Z. Xu, and Z. Shi, "An improved car-following model considering the immediately ahead cars velocity difference," *Physica A Statistical Mechanics & Its Applications*, vol. 461, pp. 446–455, 2016.

[48] S. Yu and Z. Shi, "An improved car-following model considering headway changes with memory," *Physica A: Statistical Mechanics and its Applications*, vol. 421, pp. 1–14, 2015.

[49] S. Yu and Z. Shi, "An extended car-following model considering vehicular gap fluctuation," *Measurement*, vol. 70, pp. 137–147, 2015.

[50] S. Yu and Z. Shi, "Car-following model on vehicles arrival during the red phase," *Journal of Highway and Transport*, vol. 27, no. 11, pp. 93–100, 2014.

[51] X. H. Li and S. Yu, "Analysis and modeling for car-following behaviors on arrival traffic flow of signalized intersection," *Journal of Transportation Systems Engineering and Information Technology*, vol. 15, no. 2, pp. 102–108, 2015.

[52] https://www.fhwa.dot.gov/publications/research/operations/its/06135/index.cfm.

[53] D. H. Wang, P. F. Tao, S. Jin, and D. F. Ma, "Method of calibrating and validating car-following model," *Journal of Jilin University (Engineering and Technology Edition)*, vol. s1, pp. 59–65, 2011.

[54] G. Zhu and S. Kwong, "Gbest-guided artificial bee colony algorithm for numerical function optimization," *Applied Mathematics and Computation*, vol. 217, no. 7, pp. 3166–3173, 2010.